

Conceptual development of a wedge connection for offshore  
jacket foundations



P.G. Slingerland



# Conceptual development of a wedge connection for offshore jacket foundations

By

P.G. Slingerland

in partial fulfilment of the requirements for the degree of

**Master of Science**  
in Civil Engineering

at the Delft University of Technology,  
to be defended publicly on February 22, 2019 at 2:00 PM.

Supervisor:	Prof. dr. M. Veljkovic	
Thesis committee:	Prof. dr. M. Veljkovic ,	TU Delft
	Dr. ir. M.A.N. Hendriks,	TU Delft
	Dr. H. Xin	TU Delft
	Ir. J. Winkes,	Fistuca B.V.
	Ir. K.E.Y. Creusen,	Fistuca B.V.

*This thesis is confidential and cannot be made public until February 16, 2024.*

An electronic version of this thesis is available at <http://repository.tudelft.nl/>.



## Abstract

More offshore wind projects are being developed. Shallow locations are more occupied and a tendency to deeper water and to larger wind turbines is seen. These create more bending moment which can be more easily resisted by jacket substructures.

The state of the art installation process of a jacket is as follows. The foundation piles are driven into the seabed. The jacket leg is installed by sticking a stabbing cone into the stick-up length of the foundation pile and fill the space between the cone and the pile with grout. In this situation a lot of grout, steel and installation time are used. An alternative connection could be a wedge connection which is considered in this thesis.

A wedge connection consists of four parts: jacket leg, connector element, wedges and foundation pile. The challenge to apply this connection to jackets is to overcome the installation tolerances. Due to the inaccuracy of the driving of the foundation piles, the holes in the jacket legs and the foundation piles do not align and the wedges cannot be installed. The installation tolerances consist mainly of center-to-center distance, pile verticality and a vertical tolerance. The maximum translational tolerances are 75 millimeter while the maximum rotational tolerance is maximum 0.83 degrees.

23 different concepts have been developed to deal with the installation tolerances. All the concepts have some drawbacks and do not fully solve the problem without downsides. The magnitude of the installation tolerances is therefore reduced and from a multi-criteria analysis a screw thread connection is proposed. The advantages of the screw thread connection are: a reduced amount of material, no grout is required and the installation time of the jacket to foundation pile connection can be reduced up to 75 percent.

The screw thread connection overcomes the vertical tolerance and the tolerance around the longitudinal axis of the foundation pile by rotation of the connector element. In case of an pile inclination, the connector element and the foundation pile do not fully align and a gap remains in between them. By applying a preloading force to the connection it is still not possible to close this gap. The space between the connector element and the foundation pile has to be filled with an epoxy resin.

The screw thread connection does fulfill the requirements for the ultimate limit state based upon hand calculations for net stresses, bending stresses and contact stresses. The fatigue limit state of the wedge connection meets the requirements. Only the fatigue limit state of the screw thread does not fulfill the requirements based upon a hand calculation.

The three largest issues of the screw thread connection are the fabrication of the screw thread profile, the fatigue in the screw thread and the installation of the epoxy resin between the connector and the foundation pile. The first step to develop the screw thread connection further is an more extensive investigation to these three issues.

## Acknowledgements

This thesis was a long project which consumed a lot of time. It was not always easy to stay patient and keep going until this report was finished. At this moment seeing the final result, I am happy with the work and I want to thank several people which helped or supported me to make this project a success.

First of all I want to thanks Jasper for helping me with this thesis and trusting me to make a conceptual proposal of a new connection and to bring it to a good result. While he had a lot of work to do, he was always prepared to help me.

Secondly I want to thank Koen for his guidance on the way. He was always willing to answer questions and guide me when Jasper was too busy to help. He did his master thesis a year ago and understood the process very well and kept always optimistic.

Thirdly thanks to the supervisors M. Veljkovic, M.A.N. Hendrix and H. Xin from the university for their feedback. Especially in the last part of this project.

Fourthly I am thankful to the entire team from Fistuca B.V. They created a great working atmosphere at the office, so that it was nice to be in the office and that I could enjoy my work.

Finally I want to thank my family and all friends which supported me during this project. Without their support the result of this thesis had not been what it is now.

## Content

Abstract.....	4
Acknowledgements.....	5
Content .....	6
List of figures.....	9
List of tables .....	10
Symbols and units .....	11
1. Introduction .....	16
1.1. Tendency in the offshore wind industry .....	16
1.2 State of the art of the jacket structure installation process .....	16
1.3 Wedge connection .....	16
1.4 Design goal and research questions .....	17
1.5 Fistuca .....	18
2. State of the art connection compared to wedge connection.....	19
2.1 Installation of the grouted connection .....	19
2.2 Disadvantages of the grouted connection.....	19
2.2.1 Sealing .....	20
2.2.2 Grout .....	20
2.2.3 Overlap of steel.....	20
2.2.4 Cleaning of the foundation pile .....	20
2.2.5 Pile gripper ring.....	21
2.3 Installation of the wedge connection .....	21
2.4 The advantages of the wedge connection.....	21
2.4.1 Material use .....	21
2.4.2 Cleaning.....	22
2.4.3 Hydraulic gripper ring .....	22
2.5 The disadvantages of the wedge connection .....	22
2.5.1. The wedge connection is only applicable to three-legged jacket.....	22
2.5.2. Challenging installation of the wedge connection and terminology .....	23
3. Inaccuracies in fabrication and installation .....	24
3.1. Ideal situation .....	24
3.2 Installation tolerances.....	24
3.3 The tolerances applied to the piles.....	25
3.3 Deflection of the foundation pile.....	27

3.3.1 Deflection of the pile during installation .....	27
3.3.2 Hand calculation .....	28
3.3.3 FEM-Model.....	28
3.3.4 Bending of the pile .....	30
3.4 Deviation of the foundation pile in the horizontal plane .....	31
3.5 Rotation angle and deflection by bending the foundation pile.....	31
4. Concepts and concept comparison.....	34
4.1 The concepts of the wedge connection.....	34
4.2 Multi-criteria analysis.....	34
4.3 Concepts comparison.....	35
4.4 Conclusion of the concept comparison .....	36
5. Structural design of the wedge connection.....	39
5.1 Description of the screw thread connection .....	39
5.2 Influence of inclination of the foundation pile on the screw thread connection.....	39
5.2.1 Larger wedges due to pile inclination.....	39
5.2.2 Initial line load in wedge .....	40
5.3 Design loads for ULS and FLS .....	40
5.4 Reduction of tolerances .....	42
5.5 Screw thread .....	42
5.6 Epoxy resin for void between the connector and the pile.....	43
5.7 Other structural components .....	43
5.7.1 Wedges .....	44
5.7.2 Difference in force on outer flange and inner flange .....	45
5.7.3 Difference in bending moment due to asymmetry .....	46
5.7.4 Compression stress in net area of the foundation pile.....	47
5.7.5 Tensile stress in net area of the foundation pile .....	47
5.7.6 Additional stress due to bending moment in the foundation pile .....	47
5.7.7 Tensile stress in net area of the connector.....	48
5.7.8 Contact stress between wedge and connector .....	48
5.7.9 Contact stress between wedge and foundation pile .....	48
5.7.10 Actuation force .....	49
5.7.11 Self-locking system.....	50
5.7.12 Distance from the central axis of the wedge to the edge of the flange .....	51
5.6 The actuation force on the connector .....	52

5.7 Results for the ultimate limit state .....	54
5.8 Fatigue limit state for screw thread connection.....	54
5.8.1 Fatigue in the wedges .....	55
5.8.2 Fatigue next to the holes in the foundation pile .....	56
5.8.3 Fatigue next to the holes of the connector .....	57
5.8.3 Fatigue in the screw thread .....	57
5.9 Results for the fatigue limit state.....	58
5.10 Closing of the gap between the connector and foundation pile .....	59
6. Discussion and recommendations .....	61
6.1 Interpretation of the results .....	61
6.2 Recommendations for further development.....	62
7. Conclusions .....	63
8. References .....	64
Appendix A: Graph to use for the displacement of the foundation pile .....	66
Appendix B: Installation loads on the screw thread connection .....	67
Appendix C: Bending beam equations.....	81
Appendix D: Utilize elasticity between the jacket leg and foundation pile .....	83
Appendix E: Reduced area and moment of inertia of the wedge .....	85

## List of figures

Figure 1 - Remittance of force of the jacket (left) and the monopile (right).....	16
Figure 2 - The wedge connection applied between the monopile (MP) and transition piece (TP).....	17
Figure 3 - Schematic overview of the grouted connection.....	19
Figure 4 - A ROV which cleans the inside of the pile.....	20
Figure 5 - Pile gripper ring.....	21
Figure 6 - Misalignment for a wedge connection for four-legged jacket.....	23
Figure 12 - Jacket structure.....	25
Figure 13 - Straightness taken as rotation.....	26
Figure 14 - Installation tolerances for all the foundation piles.....	26
Figure 15 - Maximum relative displacements of each of the foundation piles to the jacket in mm.....	26
Figure 16 - Maximum relative displacements of each of the foundation piles to the jacket due to the possible rotation of the vertical inclination of the foundation piles in mm.....	26
Figure 17 - Maximum relative displacement of each of the foundation piles to the jacket due to the three tolerance components in mm.....	26
Figure 18 - Maximum relative displacement of each of the foundation piles to the jacket which causes the largest rotation of the jacket.....	27
Figure 19 - Vertical displacements within a connection due to an inclination between the jacket leg and the foundation pile.....	27
Figure 20 - Rotation around the axis indicated in figure 18. This axis is parallel to the brace between legs 1 and 2.....	27
Figure 21 - Vertical displacement along a horizontal line of a jacket leg.....	27
Figure 22 - Jacket leg with seeker.....	28
Figure 23 - Model hand calculation for jacket piles.....	28
Figure 24 - Model of the foundation pile in the seabed.....	29
Figure 25 - Bending of the foundation pile by jacket leg.....	30
Figure 26 - Top view of a foundation pile installed at very accurately (left) and a foundation pile with a deviation of 50 mm to the right (right).....	31
Figure 27 - Pile top rotation and the subsequently deviation in the center-to-center distance.....	31
Figure 28 - Model to calculate the deflection and pile tip rotation of the foundation piles.....	32
Figure 30 - The scores of the multi-criteria analysis given in a column graph.....	36
Figure 32 - Foundation piles are driven into the seabed.....	39
Figure 33 - Difference between heights of the pile tops is measured.....	39
Figure 34 - Connector is screwed to the correct height.....	39
Figure 35 - The foundation pile and connector are aligned by the seeker.....	39
Figure 36 - Alignment of the holes in the foundation pile and connector.....	39
Figure 37 - Installation of the wedges.....	39
Figure 38 - Filling of space between connector and actuator with epoxy resin.....	39
Figure 39 - Not all the wedges can be pushed to the end (right).....	40
Figure 40 - Height difference between jacket leg and foundation pile.....	42
Figure 41 - Different screw thread profiles.....	43
Figure 46 - Locations of the epoxy resin.....	43
Figure 47 - Cross-section of the wedge at the location of the maximum bending moment.....	44
Figure 48 - Bending moment in a dowel according to figure 3.11 from Eurocode 1993-1-8.....	44
Figure 49 - Forces on the wedge and the corresponding moment diagrams.....	46
Figure 50 - Cross-sectional view of the wedge at the contact area (left) and the minimum contact area between wedge and foundation pile (right).....	48
Figure 51 - Free-body diagram of wedge.....	<b>Error! Bookmark not defined.</b>
Figure 52 - Self-locking system of the wedges.....	50

Figure 53 - Outer flange.....	51
Figure 54 - Cyclic symmetry with boundary conditions of first model .....	53
Figure 55 - Deformation of the flange during the installation of the wedge .....	53
Figure 56 - Maximum principle stress in the cross-section of the wedge connection.....	53
Figure 57 - Principle stress in the outside of the connection.....	53
Figure 58 - Maximum principle stresses at the outer flange .....	53
Figure 59 - Total deformation of the outer flange of the connection .....	53
Figure 60 - Maximum principle stress at the desired location .....	53
Figure 61 - Unity checks for the ultimate limit state.....	54
Figure 62 - Unity checks in FLS.....	54
Figure 63 - Detail category on fatigue according to Eurocode 1993-1-9.....	55
Figure 64 - Detail category on fatigue according to Eurocode 1993-1-9.....	56
Figure 65 - Graphs to determine the soil parameters.....	67
Figure 66 - Jacket structure of East Anglia one.....	68
Figure 67 - Dimensions for of the reference offshore jacket.....	69
Figure 68 - Top view of the jackets with the current and the wave direction in two situations .....	73
Figure 69 - Equivalent drag diameter (left) and equivalent inertia diameter (right).....	74
Figure 70 - Equivalent drag diameter (left) and equivalent inertia diameter (right).....	74
Figure 71 - Circular motion of water molecules over depth.....	75
Figure 72 - Horizontal velocity profile over water depth .....	76
Figure 73 - Maximum current at water surface of the North Sea during average tide in knots.....	77
Figure 74 - The horizontal velocity of the current profile at the location of the jacket .....	77
Figure 75 - Total horizontal water profile at the location during installation .....	78
Figure 76 - Different k-values for different materials (DNV GL, 2017a).....	78
Figure 77 - Graph to determine the Cd -coefficient.....	79
Figure 78 - Horizontal loads on jacket situation 1 (left) and for situation 2 (right) .....	80
Figure 79 - Bending beam equations .....	81
Figure 80 - Bending beam equations .....	82
Figure 81 - Connection with deformation from elasticity .....	83
Figure 82 - 40 mm between pile edge left and right.....	83
Figure 83 - The bending beam equation for the displacement in the leaf spring .....	83
Figure 84 - The upper and lower limits for the thickness and length of the spring.....	84
Figure 85 - Shear area at the critical location in the wedge .....	85

## List of tables

Table 1 - Pile installation tolerances.....	24
---	----

Table 2 - Pile geometry tolerances .....	24
Table 3 - Pile dimensions.....	25
Table 4 - Horizontal force which is needed to deflect the foundation pile 75 mm .....	30
Table 5 - Multi-criteria analysis data for all the concepts .....	36
Table 6 - The four design load cases for the wedge connection in a jacket leg .....	40
Table 7 - The maximum axial stress in tension/compression for the different diameters of the foundation pile .....	41
Table 8 - Properties and tolerances of the foundation pile in the current and new situation .....	42
Table 10 - Properties of reinforced- and unreinforced resin .....	43
Table 11 - Part of table 3.4 of Eurocode 1993-1-8.....	51
Table 12 - Unity checks in ULS for the screw thread connection .....	54
Table 13 - Results for the fatigue limit state.....	58
Table 14 - The maximum allowable preload for several components of the wedge connection for different thicknesses of the foundation pile .....	60
Table 15 - The maximum preloading force of the gap and the maximum height of the closable gap .....	61
Table 16- Dimensions of the jacket.....	71
Table 17 - Weight of several components of the jacket structure .....	71
Table 18 - Equivalent diameters for the members of the jacket in situation 1 .....	73
Table 19 - Equivalent diameters for the jacket in situation 1 in numbers .....	73
Table 20 - Equivalent diameters for the members in situation 2.....	74
Table 21 - The equivalent diameters for situation 2 in numbers .....	74
Table 22 - Forces and maximum bending resistance .....	80

## Symbols and units

$a$	Wave amplitude	[m]
$a_{in,fl}$	Center to center distance inner flange to pile	[mm]

$a_{out,fl}$	Center to center distance outer flange to pile	[mm]
$A$	Soil parameter for static loading	[-]
$A_{align}$	Cross-sectional area of aligners	[mm <sup>2</sup> ]
$A_{con,wedge}$	Contact area between wedges and connector	[N/mm <sup>2</sup> ]
$A_{cont,wedge,pile}$	Contact area between wedges and foundation pile	[mm <sup>2</sup> ]
$A_{full}$	Whole Cross-sectional area of the pile (including air)	[m <sup>2</sup> ]
$A_{full,wedge}$	Circular cross-sectional area of the wedge	[mm <sup>2</sup> ]
$A_{flanges}$	Cross-sectional area of flanges of connector	[mm <sup>2</sup> ]
$A_{in,fl}$	Area of the outer flange of the connector	[mm <sup>2</sup> ]
$A_{net,pile}$	Net area of foundation pile	[mm <sup>2</sup> ]
$A_{out,fl}$	Area of the outer flange of the connector	[mm <sup>2</sup> ]
$A_{pile}$	Cross-sectional area of the pile	[mm <sup>2</sup> ]
$A_{wedge}$	Cross-sectional area wedge	[mm <sup>2</sup> ]
$b$	Width of 1 meter	[mm]
$b_0$	Width of the jacket at the bottom braces	[m]
$b_{N_b}$	Width of bay number $N_b$	[m]
$b_{net,seg}$	Distance between the holes	[mm]
$c_{pile}$	Circumference of foundation pile	[-]
$C_D$	Drag coefficient	[-]
$C_M$	Inertia coefficient	[-]
$d$	Water depth	[m]
$d_0$	Diameter of hole in connector/foundation pile	[mm]
$d_{fl,con}$	Thickness of the flange of the connector	[mm]
$d_{pile}$	Thickness of the foundation pile	[mm]
$D$	Damage	[-]
$D_{br,d}$	Diameter of diagonal braces	[m]
$D_{br,h}$	Diameter of horizontal braces	[m]
$D_{conn,tower}$	Diameter of connection jacket structure and tower	[m]
$D_{eq,side1}$	Equivalent diameter with wave loading from side 1	[m]
$D_{in,con}$	Inner diameter of connector	[mm]
$D_{out,con}$	Outer diameter of connector	[mm]
$D_{pile}$	Outer diameter of the foundation pile	[mm]
$D_{pile,in}$	Inner diameter of the foundation pile	[mm]
$D_{wedge}$	Diameter of the wedge	[mm]
$E$	Young's modulus of steel	[GPa]
$f_y$	Yield strength of steel	[MPa]
$f_u$	Ultimate strength of steel	[MPa]
$F_{actutate}$	Required force from actuator to preload wedges	[N]
$F_{actutator}$	Force feasible from actuator to preload wedges	[N]
$F_{axial}$	Axial force on foundation pile	[kN]
$F_{Buoyancy}$	Buoyancy force	[N]
$F_{current,waves}$	Horizontal load due to current and waves	[N]
$F_{b,Ed}$	Applied force at the outer flange of the connector	[N]
$F_{b,Rd}$	Bearing resistance of the outer flange of the connector	[N]
$F_{b,Rd,pile}$	Bearing resistance of the foundation pile	[N]
$F_D$	Drag force	[N]
$F_{Ed,comp}$	Compressive load on the connection in the ultimate limit state	[N]
$F_{Ed,tension}$	Tensile load on the connection in the ultimate limit state	[N]
$F_{fr,wedge}$	Friction force developed around the wedge due to preloading	[N]
$F_{hor,pre}$	Required load from actuator to overcome only tension	[MN]

$F_I$	Inertia force	[N]
$F_{Morison}$	Morison force	[N]
$F_{net,selfw}$	Buoyancy subtracted from self-weight jacket per leg	[MN]
$F_{spatial}$	Horizontal force due to self-weight of jacket structure	[MN]
$F_{torque,align}$	Force in aligners due to torquing force to rotate the connector	[kN]
$F_{v,Ed}$	Applied shear to the wedge	[kN]
$F_{v,Rd}$	Shear resistance of wedge	[kN]
$g$	Gravitational acceleration	[m/s <sup>2</sup> ]
$h$	Height of the stabbing cone	[m]
$h_{blade}$	Thickness of elastic connection	[m]
$h_{conn,tower}$	Height of turbine foot connected to jacket	[m]
$h_{flange}$	Height of flanges of connector	[mm]
$h_{Nb}$	Height of bay number $N_b$	[m]
$h_{pitch}$	Pitch of the screw threads	[mm]
$h_{tot,bays}$	Height of all the bays	[m]
$h_{wedge}$	Distance of wedge from the middle of circle to inclined plane	[mm]
$H$	Depth below the seabed	[m]
$H_{jacket}$	Height from bottom brace to the top of the jacket	[m]
$H_{wave}$	Wave height	[m]
$I_{blade}$	Second moment of inertia of the blade per meter	[mm <sup>4</sup> ]
$I_{flange}$	Second moment of inertia of flanges connector	[mm <sup>4</sup> ]
$I_{full,wedge}$	Second moment of inertia of round wedge	[mm <sup>4</sup> ]
$I_{leg}$	Second moment of inertia of the jacket leg	[mm <sup>4</sup> ]
$I_{pile}$	Second moment of inertia of the foundation pile	[mm <sup>4</sup> ]
$I_{wedge}$	Second moment of inertia of the wedge	[mm <sup>4</sup> ]
$l_{actuator}$	Half the length of the flanges of the actuator	[mm]
$l_{blade}$	Length of elastic connection	[m]
$l_{gap}$	Length of gap between foundation pile and connector	[mm]
$l_{max,blade}$	Upper bound of elastic connection	[mm]
$l_{min,blade}$	Minimum length of elastic connection	[mm]
$L$	Diameter of members	[m]
$L_{jacket}$	Length of jacket leg between connection and lowest brace	[m]
$L_{leg}$	Length of jacket leg	[m]
$L_{br,d}$	Length of diagonal braces	[m]
$L_{br,h}$	Length of horizontal braces	[m]
$L_{stick-up}$	Length of pile above seabed	[m]
$k$	Surface roughness	[m]
$k$	Wave number	[1/m]
$k_1$	Coefficient for flange resistance of connector	[-]
$k_{flange}$	Stiffness of flanges of connector	[N/mm <sup>2</sup> ]
$k_{shell,fp}$	Stiffness of the foundation pile	[N/mm <sup>2</sup> ]
$k_{shell,jl}$	Stiffness of jacket leg	[N/mm <sup>2</sup> ]
$k_{py}$	Initial modulus of subgrade reaction	[kN/m <sup>3</sup> ]
$m$	Exponent in the S-N curve	[-]
$m_a$	Weight of structural jacket member per meter	[kg]
$m_{jacket}$	Ratio between the bays of the jacket	[-]
$M_{circ,con}$	Circumferential bending moment of foundation pile	[kNm]
$M_{Ed,pile}$	Applied bending moment on the pile	[kN]
$M_{Ed,wedge}$	Applied bending moment on wedge	[Nmm]
$M_{max,blade}$	Maximum allowable moment in elastic connection	[Nmm]

$M_{RD,wedge}$	Maximum bending resistance of wedge	[Nmm]
$n$	Expected number of cycles during lifetime	[-]
$N$	Allowable number of cycles during lifetime	[-]
$N_{align}$	Number of aligners at foundation pile	[-]
$N_b$	Number of bay	[-]
$N_c$	Reference number of cycles	[-]
$N_r$	Design life time expressed as number of cycles	[-]
$N_{wedges}$	Number of wedges in the foundation pile	[-]
$p_2$	Center to center distance between holes	[mm]
$p_{actuator}$	Maximum pressure delivered from the actuator	[N/mm <sup>2</sup> ]
$p_u$	Ultimate soil resistance	[kN/m]
$Re$	Reynolds number	[-]
$r_{A,wedge}$	Reduction factor of cross-sectional area of wedge	[-]
$r_{buoy}$	Reduction factor for buoyancy force	[-]
$r_{in}$	Ratio of inner area to area of connector	[-]
$r_{out}$	Ratio of outer area to area of connector	[-]
$r_{out/in}$	Ratio of outer area to inner area of the connector	[-]
$r_{W,wedge}$	Reduction factor of moment of inertia of wedge	[-]
$R_{pile}$	Outer radius of the foundation pile	[mm]
$R_{mid,pile}$	Radius of the foundation pile at middle of the wall	[mm]
$t_{actuator}$	Wall thickness actuator	[mm]
$t_{annulus}$	Thickness of the annulus	[mm]
$t_{conn,tower}$	Equivalent thickness connection jacket to tower	
$t_{jl}$	Wall thickness of jacket leg	[mm]
$u_{h,rot}$	Horizontal displacement of connection due to tilt of the pile	[mm]
$T$	Wave period	[s]
$T_{con-jl}$	Maximum torqueing moment between connector and jacket leg	[kNm]
$T_{con-pile}$	Maximum torqueing moment between connector and pile	[kNm]
$T_{total}$	Maximum torqueing moment to rotate connector	[kNm]
$u_v$	Vertical deviation pile edge to middle pile	[mm]
$v$	Horizontal velocity of water	[m/s]
$\dot{v}$	Horizontal acceleration of water	[m/s <sup>2</sup> ]
$v_{c,tide}$	Tidal current velocity	[m/s]
$\nu_{water}$	Kinematic viscosity of water	[m <sup>2</sup> /s]
$V_{epoxy-resin}$	Required volume of epoxy resin	[m <sup>3</sup> ]
$V_{grout}$	Volume of grout in a stabbing cone	[m <sup>3</sup> ]
$V_{jacket,bel,wat}$	Volume of jacket under water	[m <sup>3</sup> ]
$V_{steel,cone}$	Minimum amount of steel of the stabbing cone	[m <sup>3</sup> ]
$W_{el}$	Moment of inertia of wedge	[mm <sup>3</sup> ]
$W_{full,wedge}$	Moment of inertia of round wedge	[mm <sup>3</sup> ]
$W_{pile}$	Moment of inertia of pile	[mm <sup>3</sup> ]
$z_{max}$	Maximum distance from center of wedge	[mm]
$w_0$	Deviation of foundation pile in horizontal plane	[mm]
$\alpha$	Inclination of the wedge	[degree]
$\alpha_b$	Coefficient for bearing resistance of flange connector	[-]
$\alpha_{c,tide}$	Coefficient for the current profile	[-]
$\beta$	Angle between the contact surface and center of wedge	[degree]
$\gamma$	Effective soil weight	[kN/m <sup>3</sup> ]
$\gamma_{m0}$	Reduction factor yield strength of steel	[-]
$\gamma_{m2}$	Reduction factor ultimate limit state of steel	[-]

$\Delta h_{l-r}$	Gap between connector and pile	[mm]
$\Delta h_{wedge,pile}$	Gap between wedge and hole in pile due to inclination	[mm]
$\Delta V$	Vertical accuracy wedge	[mm]
$\Delta \sigma_c$	Reference value of fatigue strength at $N_c = 2$ million cycles	[N/mm <sup>2</sup> ]
$\Delta \sigma_r$	Modified fatigue strength for different number of cycles	[N/mm <sup>2</sup> ]
$\theta_{jacket}$	Rotation of jacket leg at connection	[-]
$\theta_{lead}$	Lead angle	[degree]
$\theta_{odd}$	Angle of diagonal braces with horizontal	[-]
$\theta_{pile}$	Pile top rotation	[-]
$\vartheta_{jacket}$	Tilt of the jacket structure	[degree]
$\vartheta_{max}$	Maximum difference between tilt jacket structure and pile	[degree]
$\vartheta_{max,con}$	Maximum required rotation of the connector	[degree]
$\vartheta_{max,jacket}$	Maximum tilt of the jacket structure	[degree]
$\vartheta_{max,pile}$	Maximum tilt of the pile	[degree]
$\vartheta_{seeker}$	Angle of seeker to the vertical	[degree]
$\lambda$	Wave length	[m]
$\mu$	Friction coefficient of steel to steel	[-]
$\mu_{water}$	Dynamic viscosity of water	[m/s <sup>2</sup> ]
$\mu_{jacket}$	Angle from braces to wave direction	[degree]
$\rho_{water}$	Density of water	[kg/m <sup>3</sup> ]
$\sigma_{bend,act}$	Bending stress in connector due to actuator	[N/mm <sup>2</sup> ]
$\sigma_{c,pile}$	Compression stress in the foundation pile	[N/mm <sup>2</sup> ]
$\sigma_{c,net,pile}$	Compression in net section of pile	[N/mm <sup>2</sup> ]
$\sigma_{con,wedge}$	Stress between wedges and connector	[N/mm <sup>2</sup> ]
$\sigma_{cont,pile,wedge}$	Contact stress between wedges and pile	[N/mm <sup>2</sup> ]
$\sigma_{prel,con}$	Tensile stress in connector due to preloading	[N/mm <sup>2</sup> ]
$\sigma_{t,add,net,pile}$	Tension in foundation pile due to asymmetry	[N/mm <sup>2</sup> ]
$\sigma_{t,con}$	Tension stress in connector	[N/mm <sup>2</sup> ]
$\sigma_{t,max,pile}$	Maximum tension in foundation pile in net section	[N/mm <sup>2</sup> ]
$\sigma_{t,net,con}$	Tension stress in net section of connector	[N/mm <sup>2</sup> ]
$\sigma_{t,net,pile}$	Tensile stress in net section of foundation pile	[N/mm <sup>2</sup> ]
$\sigma_{wedge,max}$	Maximum tensile stress in the wedge	[N/mm <sup>2</sup> ]
$\tau_{align}$	Shear stress in aligners	[N/mm <sup>2</sup> ]
$\tau_{con}$	Shear stress next to actuator in flange of connector	[N/mm <sup>2</sup> ]
$\varphi'$	Friction angle of sand	[degree]
$\psi$	Internal wedge angle	[degree]
$\omega$	Wave frequency	[rad]

## 1. Introduction

### 1.1. Tendency in the offshore wind industry

Since humanity is realizing that fossil fuels are not unlimited available and are harmful to the environment there is a tendency to green energy. In the Netherlands the focus is on wind energy. This is logical because the area of the Netherlands consist for a considerable part of a windy North Sea. Near the coast of the Netherlands a couple of wind farms have been developed. And more wind farms will be built in the near future (Rijksoverheid, n.d.).

The current government's coalition decided that 40 percent of the energy in 2030 will be from wind turbines in the North Sea (Rijksoverheid, 2018). The total energy delivery from the North Sea was 8.33 PJ in 2016 and the total energy usage was 2119 PJ (CBS, 2017). So there is still a long way to go.

However, suitable locations for wind farms in shallow or intermediate water depth are becoming scarcer. Therefore, there is a tendency to construct wind farms in deeper water. This gives additional challenges for the substructures. Together with the increasing size of the wind turbines the substructure has to withstand a much bigger moment. Because jackets are wider at foundation

level than monopiles (figure 1) and have lower wave and current loads (Chen, Wong, Lin, Chau, & Huang, 2016), they are more suitable as substructure for deeper water and are therefore likely to be installed more in the coming years.

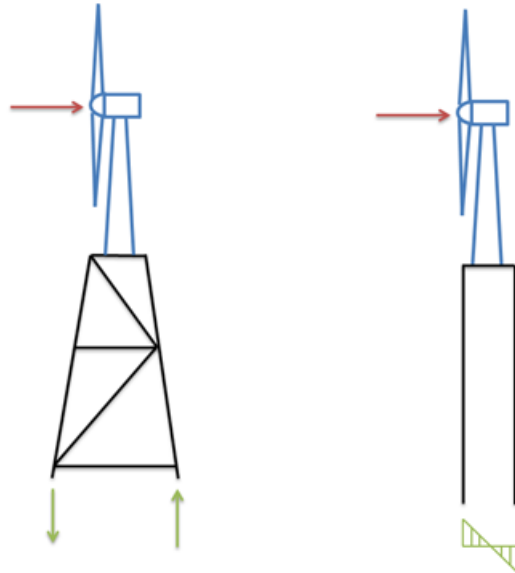


Figure 1 - Remittance of force of the jacket (left) and the monopile (right)

### 1.2 State of the art of the jacket structure installation process

A jacket is a partial underwater structure which connects the foundation piles to the wind turbine. The jacket has to be connected to the foundation piles offshore and below the water. The jacket structure itself is constructed onshore. After finishing the construction of the jacket an installation vessel will transport the jacket to the installation site. The jacket is taken from the barge, and lowered into the sea. Finally the jacket structure will be connected to the foundation piles which were already driven into the seabed. After securing of the connection between the jacket structure and the foundation piles the wind turbine can be built on top of the jacket.

### 1.3 Wedge connection

A proposed option to connect the jacket to the foundation piles is with the BLUE Wedge connection. The BLUE Wedge connection is under development by Fistuca B.V. The BLUE Wedge Connection can connect large diameter tubulars, such as a monopile (MP) and a transition piece (TP) or different segments of a wind turbine tower. A large number of holes and fasteners are evenly distributed around the circumference of the tubulars. For the MP-TP connection the

fastener consists of 2 shells and 2 wedges, which creates a vertically expanding mechanism (figure 2). The fastener is moved through over dimensioned holes in the TP and MP. Subsequently, the wedges are pulled together with a bolt. The horizontal movement expands the shells vertically, which in turn compresses the MP and TP together.

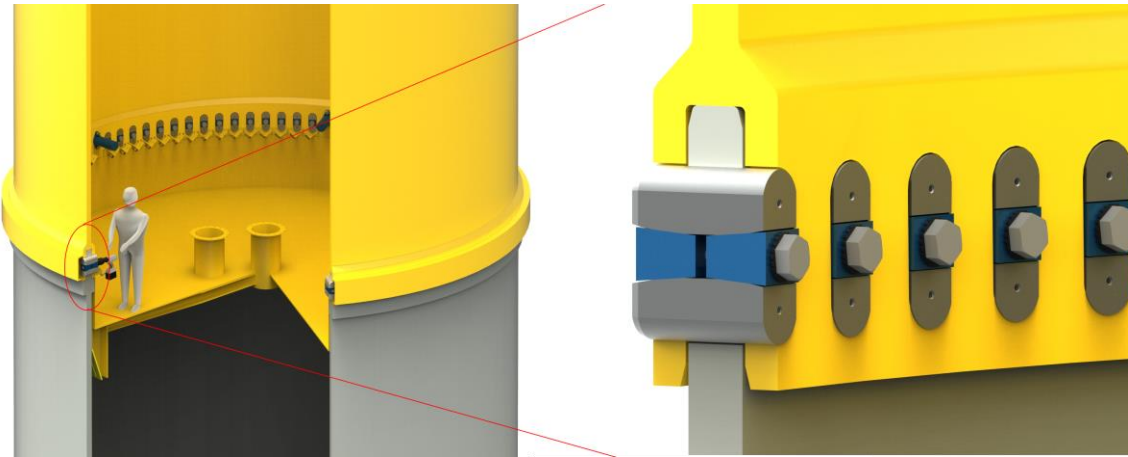


*Figure 2 - The wedge connection applied between the monopile (MP) and transition piece (TP)*

The idea is to replace bolted ring flange connection between the segments of wind turbines. The bolted connections suffer on fatigue and to prevent a failure, the bolts in the ring flange connection have to be checked every year. The wedge connection is expected to be less fatigue sensitive because no prying forces will occur. If the BLUE Wedge connection is proven to be more fatigue resistant, the wedges do not have to be checked frequently anymore on fatigue and will make the wedge connection a good alternative to connect two circular sections.

#### **1.4 Design goal and research questions**

The goal of this thesis is to develop a concept of the BLUE Wedge connection for offshore wind jackets. To reach this goal the following steps are followed. The first step is to determine the magnitude of the tolerances and the requirements for a possible wedge connection. The second step is to come up with several concepts to implement the wedge connection in offshore jackets to overcome the tolerances. This will be the most challenging part of this thesis. By using a multi-criteria analysis the most suitable concept is chosen. This concept is further developed. In order to come up with the developed concept of a wedge connection for offshore wind jackets first the design goal and research questions are set up.

Following the design goal of the thesis the main question of this thesis which has to be answered is: Is there a possibility to connect offshore wind jackets to foundation piles by using a wedge connection?

To come up with an answer to the main question the following research questions will be answered in this report. After answering all the research questions there will be enough information to give a considered answer to the main question.

For most of the research questions a chapter is used. But in some cases the research questions are too much related to each other to limit the questions to a certain chapter. Some research

questions are therefore answered partly in several chapters. The research questions are the following:

1. What is a wedge connection and which issue(s) can be solved by applying a wedge connection in a jacket? This question answers what the wedge connection is, where it is applied to and what the advantages of the wedge connection are. This question is partly answered in this chapter and partly in chapter 2.
2. Which connection is currently used and what are the disadvantages of that connection? This question is closely related to the first question. The wedge connection and the current grouted connection have to be investigated both in order to judge if the wedge connection will be a good alternative for the stabbing piles. The answer to this question is addressed in chapter 2.
3. What are the installation tolerances and degrees of freedom? Here the problem of the tolerances is addressed and specified how big the tolerances in practice are. The answer to this question is discussed in chapter 3.
4. What are possible solutions to overcome these tolerances with a wedge connection? In this chapter several concepts are globally described and a flow chart with all the concepts is given in chapter 4. Sketches of all the different concepts can be found in Appendix F.
5. What is the best solution to overcome this tolerance? Through a multi-criteria analysis the best concept is chosen. The multi-criteria analysis is also discussed in chapter 4. The concept with the highest score in the multi-criteria analysis is elaborated in research question 6.
6. How does this solution (question 4) perform in ULS and FLS? The concept which is chosen to be the best one in question 5 is dimensioned based on all the critical sections in ULS and FLS. The answer to this question is found in chapter 5.

The results and the assumptions will be discussed and evaluated in chapter 6. In this chapter also some recommendations will be given for further research or a possible other way to connect the jacket to foundation pile. Finally the conclusions which are drawn from the research questions are given in chapter 7.

## 1.5 Fistuca

Fistuca B.V. is a small company located in Delft. It is developing technologies to drive the costs of offshore wind foundations down. On one hand Fistuca is developing a BLUE Piling technology which makes use of water instead of a traditional hydraulic impact hammer. The goal of the BLUE Piling technology is to drive foundation piles quieter, more powerful and to reduce the damage during the pile driving. At the same time the company is working on the BLUE Wedge connection as a good alternative for bolted connections between monopiles and transition pieces of offshore wind turbines. In the future the wedge connection can probably also be utilized for the connections between the segments of wind turbine towers.

## 2. State of the art connection compared to wedge connection

In this chapter the state of the art connection is investigated and compared to the wedge connection. The state of the art connection for pile to jacket is the grouted connection. The installation procedure is explained in paragraph 2.1. In paragraph 2.2 the drawbacks of the grouted connection are numerated. In paragraph 2.3 a short introduction is given to the wedge connection. In paragraph 2.4 the advantages of the connection are exposed to justify the investigation of this connection while some drawbacks are given in paragraph 2.5. In section 2.6 the principle of preload for the wedge connection is explained and the load path is discussed as well.

### 2.1 Installation of the grouted connection

In the offshore wind industry pre-piling is the common procedure. The procedure of the installation of a pre-piled jacket is as follows. The foundation piles are driven into the seabed through a piling template till the pile top is between 6 and 8 meters above the seabed. The vessel with the driving equipment leaves the installation site. After some weeks to several months a large vessel with the jacket structure arrives at the installation site. Before the installation of the jacket, the inside of the foundation piles are cleaned with a remote operating vehicle (ROV). Now the jacket is lowered from the barge into the water. The jacket legs have a cone which fits spaciouly into the stick-up of the foundation pile. The cones of the jacket legs are stabbed into the foundation piles. Subsequently the space between the foundation pile and jacket leg is filled with grout. The curing of the grout takes approximately two days. Therefore a hydraulic gripper ring is integrated into the foundation pile which prevents motion of the jacket legs before the grout is cured (figure 3). After curing the tensile and compressive load are transferred from the jacket by the grout to the foundation pile through shear.

### 2.2 Disadvantages of the grouted connection

Although the grouted connection is proven to be structural reliable and seems to be a simple solution, some aspects of the grouted connection makes it expensive. The following aspects drive the costs of the grouted connection up:

- Sealing of the grout between the stabbing cone and the foundation pile
- Grout which is used to fill the annulus
- Overlap in steel of the stabbing cone and foundation pile
- Cleaning of the inner side of the foundation pile
- Long installation time or hydraulic gripper ring

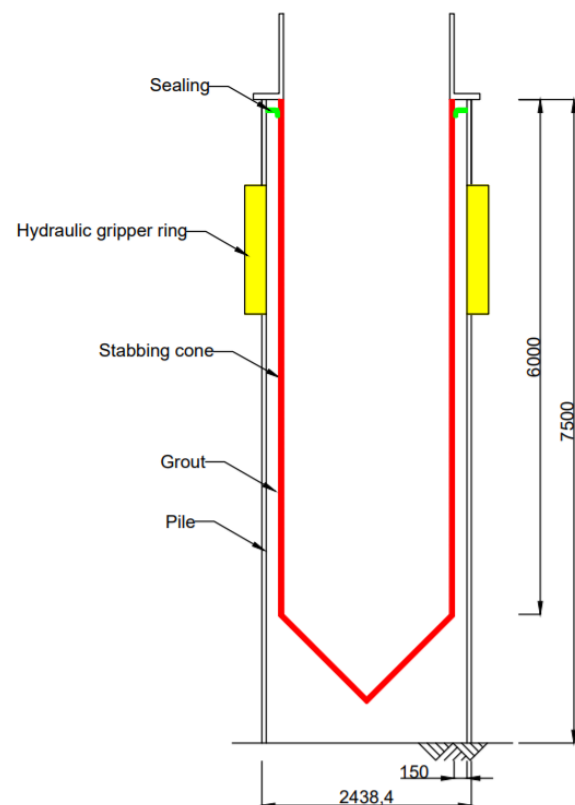


Figure 3 - Schematic overview of the grouted connection

Each of these aspects is discussed in this paragraph.

### 2.2.1 Sealing

To make a closed room for the grout a sealing is applied. The sealing is done by a ring of rubber which is fastened to the foundation pile or to the stabbing cone. By stabbing the cone into the foundation pile the whole annulus is sealed from the outside (figure 3). During the pumping of grout into the annulus the water is replaced and the heavier grout will fill the annulus.

### 2.2.2 Grout

To calculate the amount of the grout which can be saved, the thickness of the annulus has to be assumed. According to (DNVGL, 2014) the thickness of the annulus should be larger than the inner diameter divided by 45 and larger than the inner diameter divided by 10. For a 2.44 m (96 inch) diameter pile the thickness of the annulus is between:

$$51.9 \text{ mm} < t_{annulus} < 233.7 \text{ mm}$$

The width of the annulus is therefore taken to be 150 mm. The room which is filled with grout is equal to the thickness of the annulus multiplied by the length times the height of the annulus. The length of the shear connection of is 6 meter and the thickness of the annulus is 150 mm. The volume of the grout per jacket leg for a 2.44 m (96 inch) diameter pile is:

$$V_{grout} = \pi * D_{pile,in} * t_{annulus} * h \rightarrow V_{grout} = \pi * 2.19 * 0.15 * 6 = 6.2 \text{ m}^3.$$

For a three-legged jacket  $18.5 \text{ m}^3$  of grout can be saved. In this calculation the space next and below the cone are disregarded.

### 2.2.3 Overlap of steel

After the jacket leg is stabbed into the foundation pile, the steel from the stick-up of the foundation pile and the steel from the stabbing cone of the jacket leg are overlapping. When a connection can be made without stabbing cone a lot of steel can be saved. By assuming a stabbing cone with a length of 6 meters and a wall thickness of 4 cm (figure 3) for a foundation pile with a diameter of 2.44 m (96 inch) the following volume of steel can be saved:

$$V_{steel,cone} = \pi * 1.997 * 0.040 * 6 = 1.51 \text{ m}^3.$$

For a whole three-legged jacket structure this is  $4.5 \text{ m}^3$ . Which has a weight of  $7850 * 5.27 = 35459 \text{ kg}$ . That is 35.4 tons.

### 2.2.4 Cleaning of the foundation pile

To clean the inside of the foundation pile several remote operating vehicles (ROV's) are developed. Most of the ROV's have a combination of dredging and jetting. The ROV's are relatively small and can be transferred by small offshore vessels. The height of the ROV is a couple of meters and has to fit into the foundation pile so that with water jets the pile can be cleaned from the inside. An example of a ROV is shown in figure 4 (Deep C group, n.d).

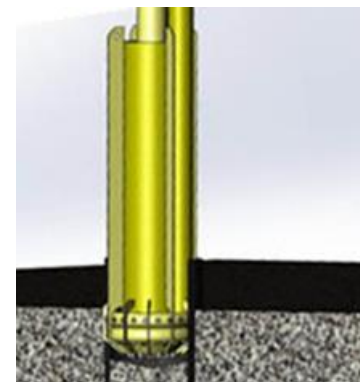


Figure 4 - A ROV which cleans the inside of the pile

### 2.2.5 Pile gripper ring

The pile gripper ring is integrated into the foundation pile to hydraulically grip the stabbing cones (figures 3 and 5). It does this to maintain stability for the subsequent installation operations such as grouting. The gripper ring protects the stabbing cone from loading and displacements and the grout can cure without being damaged. This tool can be remained gripped for extended periods, allowing for construction vessels to leave operations in bad weather, while ensuring the jacket is held in position. After curing of the grout, the gripper is fixed in the grout and will remain in the foundation pile. So for every jacket leg a hydraulic gripper ring is needed which is used only once.



Figure 5 - Pile gripper ring

## 2.3 Installation of the wedge connection

Foundation piles with holes near the pile top are driven into the seabed through a piling template. The piling stops when the pile top is between 2 and 4 meters above the seabed. After removing the piling template an installation vessel with the jacket structure arrives at the installation location. The jackets are lowered into the sea till the jacket legs touch the foundation piles. Seekers (figure 22) will guide the jacket legs to the desired position. Thereafter the holes in the jacket leg are aligned with the holes in the foundation pile by a mechanism (which is determined in this thesis). Since all the holes are aligned, the wedges can be pushed by hydraulic actuators (remotely controlled) into the aligned holes. Subsequently the wedges are fastened. Now the wedge connection is fixed to the foundation piles and the installation vessel leaves the installation site.

## 2.4 The advantages of the wedge connection

The expensive aspects of the grouted connection which are not valid for the wedge connection are the following:

### 2.4.1 Material use

The wedge connection is a slender connection. It requires less material as the grouted connection. First of all, the steel of the stabbing cone is saved. Secondly (almost) no grout is needed for the wedge connection. As a result the material costs can be reduced significantly.

### 2.4.2 Cleaning

The jacket is connected to the foundation piles a few meters above seabed. The load is transferred by wedges in the holes near the top of the foundation pile instead of shear along the inside of the pile. So only the pile top of the foundation pile at the location of the wedges has to be clean. As a result the inside of the foundation pile has not to be cleaned anymore before the installation of the jacket. This intermediate step with a smaller vessel involved can be passed over completely.

### 2.4.3 Hydraulic gripper ring

An integrated hydraulic gripper ring into the foundation pile is unnecessary and can be saved for all the three jacket legs. In case of a grouted connection where the hydraulic gripper ring is not integrated into the jacket leg, installation vessels have to stay offshore to hold the jacket at location until the grout is cured. In that case the installation time can be reduced with hours or even days by installing the wedge connection.

## 2.5 The disadvantages of the wedge connection

### 2.5.1. The wedge connection is only applicable to three-legged jacket

Consider the two following situations: In the first situation four foundation piles for an offshore wind jacket are driven into the seabed (top view left in figure 6). Three of the four piles are driven exactly into the right position while the fourth pile (most right) is driven 10 centimeters too far into the seabed. The jacket can be modelled in this case as a rigid structure. This means that in case of a rotation of the jacket structure the bottom plane of the jacket legs get a rotation as well. So in this case one of the foundation piles is driven deeper into the seabed, the bottom plane of the jacket legs will get a rotation (dashed line in figure 6) but the plain remains undistorted. Therefore not all the jacket legs can make contact anymore with the foundation piles (most left in figure 6) and the wedges cannot be installed to all the foundation piles.

In the second situation three piles for an offshore jacket are driven into the seabed (Top view right in figure 6). Two of the three foundation piles are driven very accurately away. While the third pile (most right) has a deviation of 10 centimeters too far in the sea bed. From the side view it is clear the pile tops remain in a flat plane. The plain gets only a rotation. Since the pile tops are all touching the same plane, the jacket structure will follow the inclination of this plane and all the jacket legs can be installed to the foundation piles.

The conclusion is that the wedge connection can only be applied to a three-legged jacket, unless a mechanism is found which can compensate for the difference in height between pile tips of the four legs.

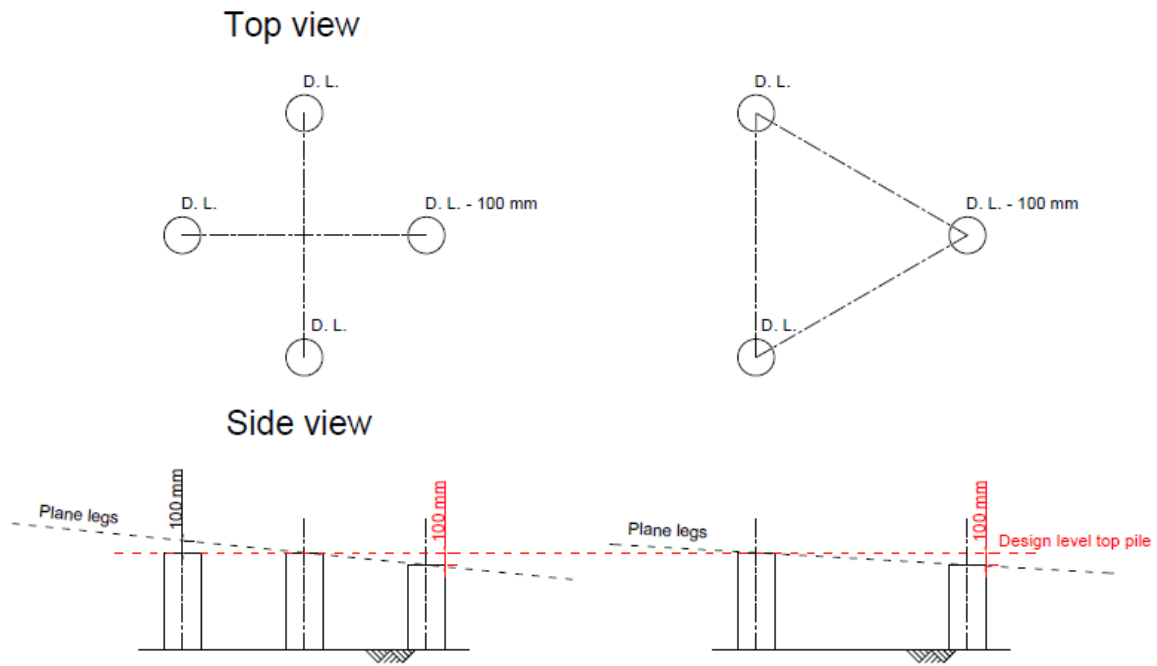


Figure 6 - Misalignment for a wedge connection for four-legged jacket

### 2.5.2. Challenging installation of the wedge connection and terminology

To connect the jacket leg with the foundation pile a mechanism is required to align the holes in the connection (chapter 3 and 4). This mechanism will exist of an additional member between a foundation pile and a jacket leg. This member is called the connector. This thesis is mainly about designing the connector. Challenges will be the installation of the connector and the installation of the wedges 40 meters below sea-level. Further on in this report the connector can be referred to as 'upper flange' and the foundation pile as 'lower flange'.

### 3. Inaccuracies in fabrication and installation

For the current grouted connection the foundation piles do not need to be installed in exactly the right position. The foundation piles are driven within certain margins to make a grouted connection possible. In this chapter the margins will be investigated to find the requirements for the concepts in the next chapter. In paragraph 3.1 the perfect conditions for installing the foundation pile are described. In paragraph 3.2 all the installation tolerances are qualified and quantified. In the paragraphs 3.3 to 3.5 some possible ways to tackle the tolerances are discussed. This ways can be implemented upon the concepts in the next chapter.

#### 3.1. Ideal situation

In the ideal situation the foundation piles could be installed within a millimeter accurate. In this case the holes in the foundation pile would align perfectly with the holes of the jacket leg. In that situation no connector had to be designed and the design of the wedge connection for the monopile - transition piece could be scaled and be applied to the jacket leg connection.

#### 3.2 Installation tolerances

In reality the foundation piles cannot be installed on the millimeter accurate due to soil properties, tolerances in the geometry of the foundation pile and in the piling template. Hence tolerances are applied to the installation of the foundation piles. The tolerances which are determined based on discussions with industry experts handles for 2438.4 mm (96 inch) diameter piles for the grouted connection. All the installation tolerances, geometry tolerances and pile dimensions are given in tables 1, 2 and 3.

<b>Pile Installation Tolerances</b>	

Table 1 - Pile installation tolerances

<b>Pile geometry tolerances</b>	

Table 2 - Pile geometry tolerances

Pile Dimensions	

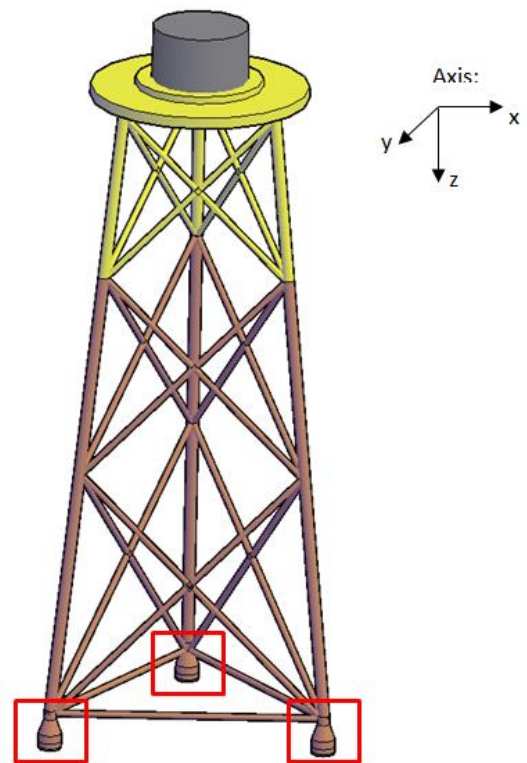
Table 3 - Pile dimensions

### 3.3 The tolerances applied to the piles

In figure 12 a jacket structure is shown. Only with the jacket legs (red framed boxes) is dealt in this report. The axes in this report are defined as in figure 12.

Some assumptions have to be made in order to apply the installation tolerances to the foundation pile. The following assumptions are made:

- ✓ The center-to-center distance between the jacket legs is 25 meter, which gives the largest possible rotation tolerance of the jacket structure.
- ✓ The connection which intercepts the tolerances is located 2.5 meter above the seabed.
- ✓ The pile straightness which is defined as xx mm per xxx mm from table 2 is taken as tilt of the pile →  $\tan(\text{xxx mm}/\text{xxx mm}) = \text{xxx}$  degrees. A sketch is shown in figure 13.
- ✓ The out of roundness is compensated by a little space between the upper and lower flanges and by the tapering of the edges of the upper flanges.



25 m  
Figure 7 - Jacket structure

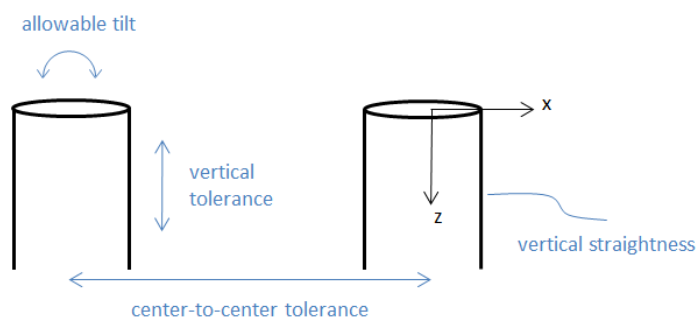


Figure 8 - Straightness taken as rotation

Figure 9 - Installation tolerances for all the foundation piles

The tolerances can be divided into three components

(figure 14):

- ✓ Relative displacement between a foundation pile and jacket structure in z-direction (vertical tolerance)
- ✓ Relative displacement between a foundation pile and jacket structure in the xy-plane (center-to-center tolerance)
- ✓ Tilt of the foundation pile tip: (allowable tilt + pile straightness)

By substituting the applicable numbers (the green lines from table 1) into these three tolerances, the following results for all the tolerances are obtained:

- ✓ Vertical tolerance:  $\pm$  xxx mm for each of the foundation piles
- ✓ Center-to-center tolerance:  $\pm$  xxx mm for each of the foundation piles
- ✓ Allowable tilt + pile straightness:  $\pm$  xxx degrees for the tilt and  $\pm$  xxx degrees for the pile straightness

In the figures below the installation tolerances are visually applied to the jacket legs. In different figures the different tolerances are shown. In figure 15 the maximum translational tolerances according to table 1 for each of the foundation piles are visualized.

Figure 10 - Maximum relative displacements of each of the foundation piles to the jacket in mm

In figure 15 only the translational tolerances were shown. However, the pile rotation causes also a horizontal translation of the pile top. The maximum rotation of each of the jacket legs is the sum of the allowable tilt and the pile straightness. From tables 1 and 2 and the assumption of the pile straightness, the maximum rotation of the foundation pile is 0.56875 degrees. The stick-up length of each of the foundation piles is 2.5 meter. So the maximum horizontal displacement in the xy-plane for each of the foundation pile tops (figure 16) due to the rotation of foundation piles is equal to:

$$u_{h,rot} = \tan(0.56875) * 2.5 = 25 \text{ mm}$$

Figure 11 - Maximum relative displacements of each of the foundation piles to the jacket due to the possible rotation of the vertical inclination of the foundation piles in mm.

The maximum possible relative displacements between the foundation piles and the jacket legs from the three main directions are given in figure 17.

Figure 12 - Maximum relative displacement of each of the foundation piles to the jacket due to the three tolerance components in mm

Now consider only the displacements in the z-direction. The maximum positive displacement is applied to leg 1 and 2. The maximum negative displacement is applied to leg 3. In figure 18 the displacements are shown. These displacements cause a rotation of the jacket structure around the rotation axis.

*Figure 13 - Maximum relative displacement of each of the foundation piles to the jacket which causes the largest rotation of the jacket*

The maximum rotation of the jacket structure is equal to:

$$\vartheta_{jacket} = \tan^{-1}\left(0.1/25 * \frac{\sqrt{3}}{2}\right) = 0.2646 \text{ degrees}$$

*Figure 15 - Rotation around the axis indicated in figure 18. This axis is parallel to the brace between legs 1 and 2*

*Figure 14 - Vertical displacements within a connection due to an inclination between the jacket leg and the foundation pile*

The maximum rotational difference between the jacket leg and the foundation pile is the sum of the maximum rotation of the jacket structure and the maximum rotation of the foundation pile. The maximum rotational difference between the jacket leg and the foundation pile is:

$$\vartheta_{max} = \vartheta_{max,pile} + \vartheta_{max,jacket} \rightarrow \vartheta_{max} = xxx + xxx = xxx \text{ degrees}$$

This results in a misalignment between the holes in the jacket legs and the holes in the foundation piles. For a foundation pile diameter of 2.44 meter (96 inch), the maximum misalignment between the holes in the foundation pile and the jacket leg is:

$$u_v = \tan(\vartheta_{max}) * \frac{R_{pile}}{2} \rightarrow u_v = \tan(xxx) * xxx = xxx \text{ mm}$$

The relative displacement between the holes in the foundation pile and the holes in the jacket leg is visualized in figure 21. From this figure is clear that the maximum relative displacement is linear to the diameter of the jacket leg. For an outer diameter of 2.44 m (96 inch) the maximum relative displacement is xxx mm. A solution is needed to overcome all these tolerances. The concepts in the next chapter have to overcome all these tolerances.

### 3.3 Deflection of the foundation pile

*Figure 16 - Vertical displacement along a horizontal line of a jacket leg*

#### 3.3.1 Deflection of the pile during installation

An option to get rid of the horizontal translational tolerances is to bend the foundation pile by the self-weight of the jacket during the installation of the jacket. At the bottom of the jacket legs seekers are attached. A seeker is assumed to have an angle of 10 degrees with the vertical

(figure 22). By lowering the seekers into the foundation piles large spatial forces are developing (figure 25). These forces have to be large enough to bend the foundation piles in the desired position.

The maximum horizontal tolerance for a 2.4384 m (96 inch) diameter pile with 2.5 meter stick-up length is 75 mm according to paragraph 3.2. So in the worst case scenario the top of the foundation pile has to be deflected 75 millimeter. The required force to bend the foundation pile back to the desired position can be calculated. This will be done in two ways. The first way is by using a clamped pile which has a length of at 4.5 to 6 times the pile diameter plus the stick-up length (figure 23). With the bending beam equations in appendix C the required force can be determined. The second case is by using a FEM-model in which the soil is represented by horizontal springs with different stiffness's.

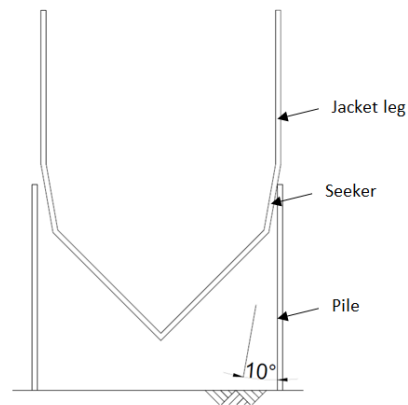


Figure 17 - Jacket leg with seeker

### 3.3.2 Hand calculation

A larger pile diameter gives a smaller length in the bending beam equations model (J.S. Hoving, 2017b). The clamping length for jacket piles from the oil and gas industry is  $6 * D_{pile} + L_{stick-up}$ . The foundation piles for offshore wind jackets have a larger diameter than the piles for the oil and gas industry and are therefore clamped less far below the seabed. The clamping length for large jacket piles is assumed to be  $4.5 * D_{pile} + L_{stick-up}$ . The horizontal load to bend the foundation pile is assumed to be within the required load to bend a foundation pile for  $6 * D_{pile} + L_{stick-up}$  and  $4.5 * D_{pile} + L_{stick-up}$ . This gives a range for the load  $F_{horizontal}$ . The results of the FEM-model with the p-y curves are expected to be in the range of  $F_{horizontal}$ . The force which is required to bend the foundation pile is calculated from bending beam equation 2 in appendix C. The results from the hand calculations are displayed in table 4.

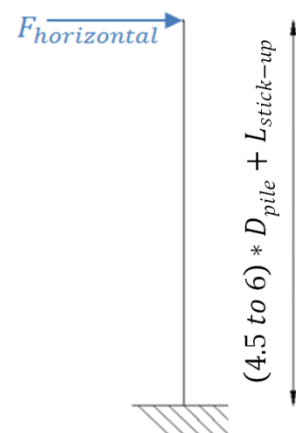


Figure 18 - Model hand calculation for jacket piles

### 3.3.3 FEM-Model

By determining the horizontal displacement, the model as shown in figure 23 is used. The foundation pile is driven up to 40 meters into the seabed. The stick-up length is 2.5 meters. The soil is modeled as linear distributed springs. The distance between each of the springs is 2 meters and each spring represents the stiffness of a 2 meter layer of ground. The lowest springs do not contribute to the deflection of the foundation pile at the top due to the length of the pile and the stiffness of the higher springs. The bottom of the foundation pile is connected with a vertical spring. This spring does not have any contribution to the horizontal deflection of the foundation pile, but is just modelled to prevent any vertical movement of the foundation pile.

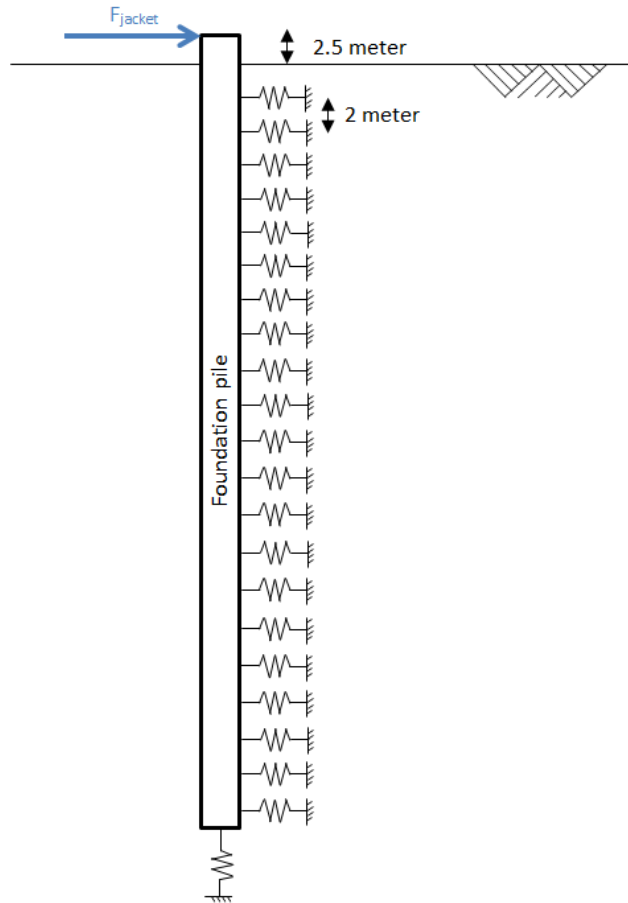


Figure 19 - Model of the foundation pile in the seabed

### P-y curves

Soil is a very inhomogeneous material with complicated properties. The young's modulus of soil is non-linear. To approach the stiffness of the soil a non-linear spring model is used. The stiffness of every spring is determined by the density of the soil and the depth. The deeper the spring is in the ground, the higher the young's modulus, the smaller the elastic strain and the higher the resistance. These properties are represented by so-called p-y curves. Thus every spring has its own p-y curve. The lateral soil resistance-deflection (p-y curve) relationship for piles in sand is defined in a study by O'Neill and Murchinson (DFI, 2013) as follows:

$$P = A * p_u * \tanh \left[ \frac{k_{py} * H}{A * p_u} * \gamma \right]$$

With:

$$p_u = \min \left( (C_1 * H + C_2 * D_{pile}) * \gamma * H; C_3 * D_{pile} * \gamma * H \right)$$

Where:

$$A = \max \left( 3.0 - 0.8 * \frac{H}{D}, 0.9 \right)$$

$$p_u = \text{ultimate resistance} \left( \frac{kN}{m} \right)$$

$\gamma = \text{effective soil weight} \left( \frac{kN}{m^3} \right)$   
 $H = \text{depht} (m)$   
 $\varphi' = \text{angle of friction of sand, (deg)}$   
 $D_{pile} = \text{pile diameter} (m)$

The coefficients  $C_1$ ,  $C_2$  and  $C_3$  are determined from figure 65 in Appendix A. All the coefficients are dependent on the friction angle of the ground. The friction angle is dependent on the type of soil. The soil is assumed to be medium dense sand. As a result a friction angle of  $32.5^\circ$  is chosen (figure 65 in Appendix A). As a result the values for the coefficients  $C_1$ ,  $C_2$  and  $C_3$  and for  $k_{py}$  are obtained. Now all the values for the p-y curves are determined. By substituting these values into the FEM-model, the required force to bend the foundation pile 75 millimeter is obtained. The results from the FEM-model are shown in table 4.

Pile diameter	Force needed to bend the foundation pile 75 mm in MN (hand calculation)	Force needed to bend the foundation pile 75 mm in MN (FEM)
1828.8 mm (72 inch)	2.17 - 4.29	3.4
2133.6 mm (84 inch)	2.38 - 4.81	3.9
2438.4 mm (96 inch)	2.55 - 5.25	4.8

Table 4 - Horizontal force which is needed to deflect the foundation pile 75 mm

From table 4 can be concluded that the result of the calculation of the FEM-model is in the range of the forces from the hand calculations. So the values from the FEM-model are reliable and are used in the next paragraph.

### 3.3.4 Bending of the pile

The bending of the pile is illustrated in figure 25. The vertical force is the self-weight minus the buoyancy of the jacket. A large spatial force is developing when the seeker touches the foundation pile due to the fact that the reaction force between the seeker and the pile is perpendicular to the surface of the seeker (figure 25).

To determine if the foundation pile can be bent 75 mm by the self-weight of the jacket during installation, the self-weight of the jacket and the buoyancy force acting on the jacket have to be determined. The self-weight of the jacket is 8.5 MN (Appendix B). The buoyancy of the jacket is equal to 4.0 MN (Appendix B). So the maximum net force downwards to the jacket legs is 4.5 MN. This is 1.4 MN per leg and with an angle of the seeker of 10 degrees with the vertical the maximum horizontal force is:

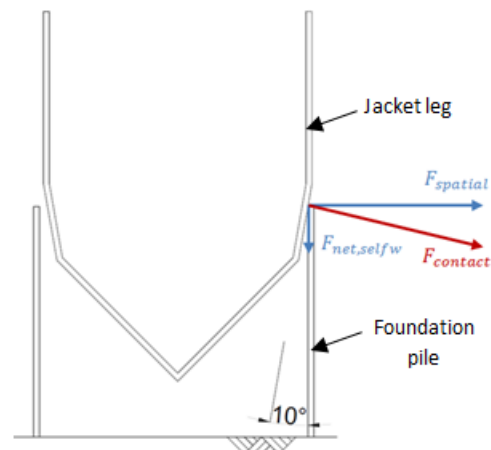


Figure 20 - Bending of the foundation pile by jacket leg

$$F_{spatial} = \frac{F_{net,selfw}}{\sin(\vartheta_{seeker})} = \frac{1.50}{\sin(10)} = 8.6 \text{ MN}$$

The horizontal force from the self-weight of the jacket is larger than the required force to bend the pile. So, the foundation pile top can be bent 75 mm with the self-weight of the jacket.

### 3.4 Deviation of the foundation pile in the horizontal plane

In figure 26 the cross-sectional view of the foundation pile and the connector is shown at the location of the holes in the foundation pile and in the connector. In figure 26 (left) the foundation pile is installed very accurately. As a result there is a perfect alignment between all the holes in the connector and the foundation pile. In figure 26 (right) the foundation pile has a deviation of 50 mm to the right. In that case the holes at location 1 and 3 do align. But the holes 2 and 4 are not aligned anymore. In this case not all the wedges can be installed. So the deviation of the pile top cannot be intercepted by the space between the connector and the foundation pile. This will create a misalignment between the holes in the connector and the holes in the foundation pile which are located perpendicular to the deviation of the foundation pile. Almost no space between the flanges of the connector and foundation pile is therefore allowed and in case of a deviation of the foundation pile, the pile has to be bent to fit in the connector.

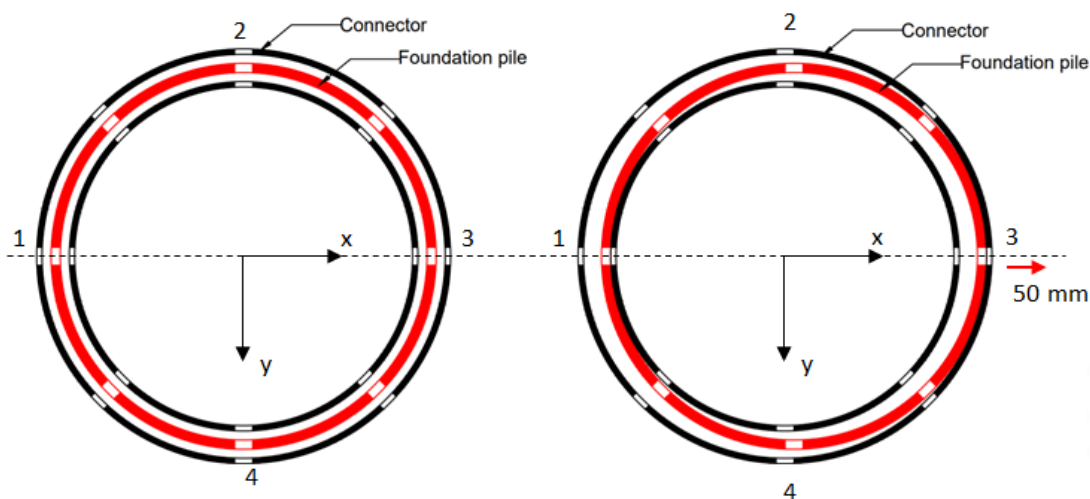


Figure 21 - Top view of a foundation pile installed at very accurately (left) and a foundation pile with a deviation of 50 mm to the right (right)

### 3.5 Rotation angle and deflection by bending the foundation pile

In this paragraph is investigated if it is possible that by bending foundation piles to the correct position in the xy-plane, as described in paragraph 3.3, the rotation of the pile top and the rotation of the jacket leg are the same.

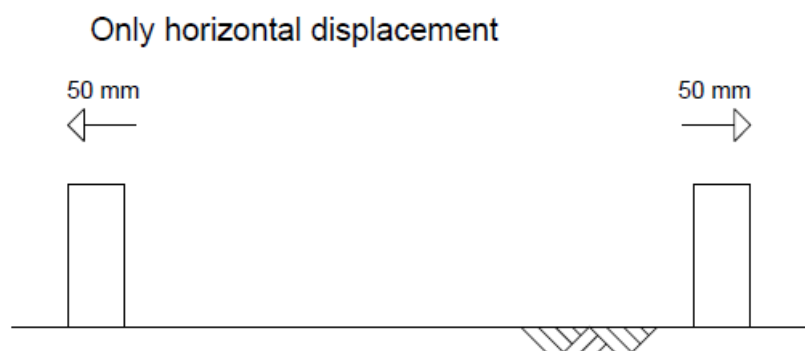


Figure 22 - Pile top rotation and the subsequently deviation in the center-to-center distance

To investigate this question the following situation is considered. Two foundation piles are assumed to have a deviation of 50 mm (figure 27) relative to the jacket legs. By forcing the foundation piles with the jacket legs into the right position as discussed in paragraph 3.4, the foundation piles and the jacket legs will deflect.

The requirement to connect the jacket legs with the foundation piles is that the rotation at the bottom of the jacket legs has to be equal to the rotation of the pile tops. While in the xy-plane (figure 12) the jacket legs and the foundation piles have the same location, so that the foundation pile fits into the connector.

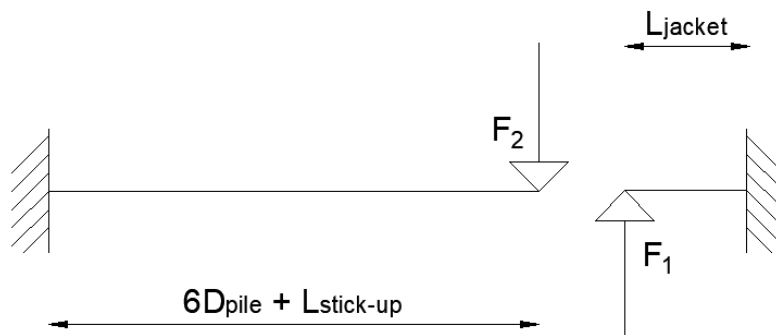


Figure 23 - Model to calculate the deflection and pile tip rotation of the foundation piles

The modelling of the jacket leg is done as shown in figure 28. The lengths of the foundation pile and jacket leg are determined. The pile has an outer diameter of 2438.4 mm (96 inch) and a wall thickness of 50.8 mm (2 inch). For the jacket leg the diameter is assumed to be 2.0 meters with a wall thickness of 40.0 mm. The stick-up length to the connection is 2.5 meter and the length from the connection to the lowest horizontal brace is 2 meters. At this location the jacket leg is fixed in this model.

With the help of the bending beam equation 2 in appendix C the following equations have to be solved:

$$w_1 + w_2 = \frac{F_1 l_1^3}{3EI_1} + \frac{F_2 l_2^3}{3EI_2} = w_0$$

$$\theta_1 = \frac{F_1 l_1^2}{2EI_1} = \theta_2 = \frac{F_2 l_2^2}{2EI_2}$$

In which:

$$l_1 = L_{jacket} = 2 \text{ meter}, l_2 = 6D_{pile} + L_{stick-up} = 17.13 \text{ meter}$$

$$F_1 = F_2 = F_{spatial}, I_1 = I_{pile} \text{ and } I_2 = I_{leg}$$

$$\theta_1 = \theta_{pile}, \theta_2 = \theta_{jacket}$$

By substituting the values in equation  $w_1 + w_2 = w_0$ , with  $w_0 = 50 \text{ mm}$  and with the knowledge that  $F_1 = F_2$  according to Newton's third law, the forces  $F_1$  and  $F_2$  are equal to 1.75

MN. By substituting this force in the second equation, the values for  $\theta_1$  and  $\theta_2$  are respectively 0.00436 and 0.000136. These two rotations are not equal and the holes in the jacket leg and the holes in the foundation pile do not align by bending the foundation pile with the jacket leg.

So these formulas cannot be satisfied both for all the possible stiffness's and lengths of both beams in the beam model. This leads to the conclusion that for most diameters and wall thicknesses the foundation pile and the jacket leg have a different rotation angle at the connection. Thus by bending the foundation pile into the right position, a mechanism has to be applied to overcome the difference in rotation between the jacket leg and the foundation pile.

## 4. Concepts and concept comparison

A whole Scala of possible solutions to overcome the tolerances have been considered. In paragraph 4.1 a flow chart with all the different concepts is shown. A multi-criteria analysis is applied in paragraph 4.2 and 4.3 to the most applicable concepts from the flow chart. The conclusion is drawn in paragraph 4.4 and the concept with the highest score from the multi-criteria analysis is elaborated further in the next chapter.

### 4.1 The concepts of the wedge connection

In order to show the development of the different concepts a flow chart of the process is composed. From top to bottom and from the left to the right the numbers of each of the concepts increases. The increase of the numbers does not show an exact chronological order, but in headlines this is the case. From all of the concepts a drawing of a cross-section in the middle of the pile is added in appendix F. The way to overcome the tolerances for all this connections is described in Appendix F as well.

### 4.2 Multi-criteria analysis

To apply a multi-criteria analysis all the concepts in the flow chart are divided into four groups (black framed boxes in figure 29). For each of the groups the most feasible concept is chosen, analyzed in the multi-criteria analysis and compared to the current connection. The four connections which are compared to each other and to the current connection are the concepts xxx, xxx, xxx and xxx. To understand the motivation for the scores in the multi-criteria analysis, a short description of the concepts is given here.

The concepts are rated on six category classes. The concepts can earn 1 to 5 points at all the different categories. The score appointed to a concept for all categories is subjective, because they are given with limited knowledge. The more a concept suffices the criteria, the higher the score on a concept. The scores of the 6 criteria are added together. So the maximum possible score for each of the concepts is 30 points. The concept with the highest total score suffices the best the categories on which the concepts are graded. And this concept is therefore selected as concept which is elaborated in this report. The six categories are explained below.

#### 1. Grout used

The use of grout is a solution that works. However, due to sealing and cleaning of the piles, grout has a negative image in the industry and solutions without the use of grout are preferred.

#### 2. Technical feasibility

The concept should be technical feasible. Some concepts are based upon a new technology, for most of the concepts it is not completely clear how technical feasible they are.

#### 3. Economical material use

In the current connection a lot of grout and steel is used. The idea of the new connection is to reduce the amount of material. Especially the use of grout and steel can be reduced and a lot of material costs can be saved.

#### 4. Short installation time

The installation time is an important aspect. A long installation time means a long time offshore for the installation vessels. Installation vessels with the personal offshore are expensive. Therefore the hours offshore for the installation vessels should be limited as much as possible.

#### 5. Simple solution

A simple solution means that the solution is easy to understand and implement. Also, that no complicated mechanisms are introduced to transfer the force and the concept is straightforward and clear to explain.

#### 6. Risk-free solution

By applying a new solution there will always be an opportunity on unforeseen negative issues. To reduce the risk, extra tests and measures have to be taken to increase the certainty that the connection works. This will increase the costs of the solution.

### **4.3 Concepts comparison**

In this paragraph the scores for all the concepts and the current connection are determined. The motivation for each of the scores is given. At the end of the paragraph the scores are shown in a table and visualized in a graph. The motivation for the scores of the concepts is as follows.

#### 1. Grout used

#### 2. Technical feasibility

#### 3. Economical material use

#### 4. Short installation time

#### 5. Simple solution

#### 6. Risk-free solution

#### 1. Grout used

#### 2. Technical feasibility

#### 3. Economical material use

#### 4. Short installation time

#### 5. Simple solution

#### 6. Risk-free solution

#### 1. Grout used

#### 2. Technical feasibility

#### 3. Economical material use

#### 4. Short installation time

#### 5. Simple solution

#### 6. Risk-free solution

#### 1. Grout used

#### 2. Technical feasibility

#### 3. Economical material use

#### 4. Short installation time

#### 5. Simple solution

#### 6. Risk-free solution

#### 1. Grout used

#### 2. Technical feasibility

#### 3. Economical material use

- 4. Short installation time
- 5. Simple solution
- 6. Risk-free solution

**Final scores for the concepts**

The final score for all the different concepts and the current connection are given in table 5.

Concept	Grout used	Technically feasible	Economical material use	Short installation time	Easy solution	Risk-free solution	Total
	1	5	2	1	4	4	17
	2	4	3	3	4	3	17
	5	1	4	4	2	2	18
	5	3	4	3	4	2	21
	5	2	4	2	4	1	18

*Table 5 - Multi-criteria analysis data for all the concepts*

To make the scores more visual the results of the multi-criteria analysis are given in figure 30.

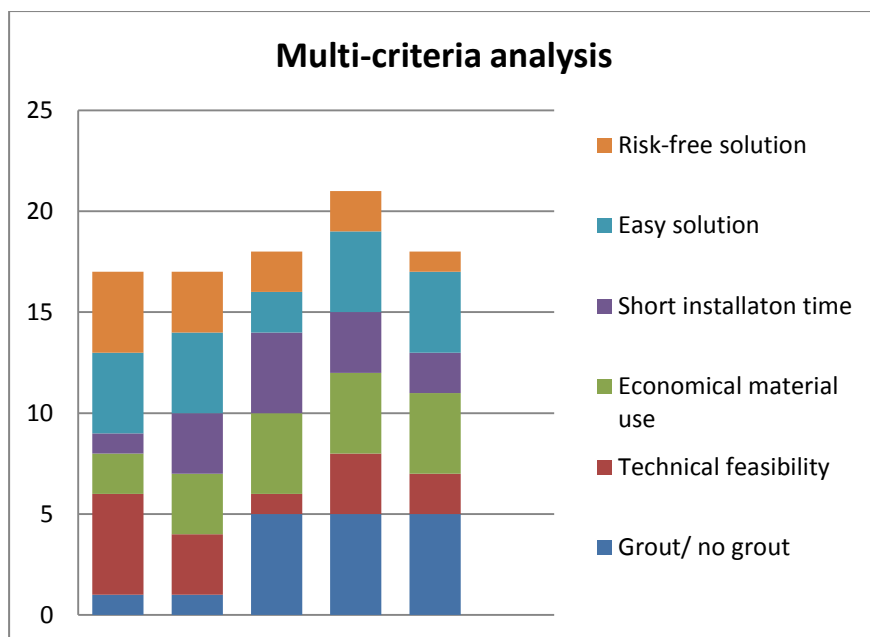


*Figure 24 - The scores of the multi-criteria analysis given in a column graph*

**4.4 Conclusion of the concept comparison**

The screw thread connection gets the highest score and is therefore further analyzed in this thesis. The total scores from all the concepts are relatively close. This indicates that no perfect solution is found and all the concepts including the screw thread connection have drawbacks. The concepts have all a slightly higher score than the current solution. The grouted connection

has the advantage that it is currently operative. It has already been proven to be a functioning connection while the other solutions still have to be developed. However, the screw thread connection makes the biggest opportunity to be competitive to the grouted connection and replace this connection based on the results of the multi-criteria analysis.



## 5. Structural design of the wedge connection

In this chapter the screw thread connection is checked for the ultimate limit state and fatigue limit state. In paragraph 5.1 the screw thread connection is described in more detail. In paragraph 5.2 the influence of the pile inclination on the screw thread connection is described. The stresses in the foundation pile are determined in paragraph 5.3. In paragraph 5.4 new installation tolerances are introduced. In the paragraphs 5.5 to 5.7 the ultimate limit state of the screw thread connection is checked. In the paragraphs 5.8 and 5.9 is determined if the screw thread connection fulfills the fatigue limit state. In the last paragraph is determined if the screw thread connection can be made without an epoxy resin.

### 5.1 Description of the screw thread connection

*Figure 25 - Foundation piles are driven into the seabed*

*Figure 26 - Difference between heights of the pile tops is measured*

*Figure 27 - Connector is screwed to the correct height*

*Figure 28 - The foundation pile and connector are aligned by the seeker*

*Figure 29 - Alignment of the holes in the foundation pile and connector*

*Figure 30 - Installation of the wedges*

*Figure 31 - Filling of space between connector and actuator with epoxy resin*

### 5.2 Influence of inclination of the foundation pile on the screw thread connection

In this paragraph a more detailed description is given about the screw thread connection in case of an inclination of the foundation pile.

#### 5.2.1 Larger wedges due to pile inclination

If the foundation pile is not aligned with the jacket leg, there will appear a gap between the connector and the foundation pile. As shown in figure 39 the holes in the foundation pile are lower than the holes in the connector at the location of the gap. The wedges can be only pushed into these gaps due to the wedge inclination. Without the wedge inclination it is not possible to push the wedges into these holes (figure 39 right). In the current situation this results in wedges

which stick out at the inside of the foundation pile when the holes in the foundation pile and in the connector are perfectly aligned (figure 39 left). When the holes are not aligned vertically the wedges will stick out at the outside of the foundation pile (figure 39 right). To limit the stick-out length of the wedge, the wedge angle was determined to be 10 degrees. Further is the wedge 60 millimeter longer than it should be in a situation without tilt of the foundation pile.

Figure 32 - Not all the wedges can be pushed to the end (right) due to the tilt of the foundation pile

### 5.2.2 Initial line load in wedge

The connector is always aligned with the jacket leg. The wedges are aligned with the connector. Therefore the wedges are also aligned with the jacket leg. This means that the orientation of the wedges is always horizontal. In case the foundation pile has a tilt of 0.25 degrees, the holes in the foundation piles have an orientation of 0.25 degrees. This is resulting in a small misalignment between the inclined contact surface between the wedge and the foundation pile. The maximum gap caused by the misalignment between the holes in the foundation pile and the wedges is equal to:

$$\Delta h_{wedge,pile} = \tan(\vartheta_{pile}) * t_{pile} \rightarrow \Delta h_{wedge,pile} = \tan(0.25^\circ) * 50.8 \text{ mm} = 0.22 \text{ mm}$$

This is very small. However, if the contact surface of the wedge and the contact surface of the foundation pile are not correctly aligned, a line load will occur. The contact stress between the wedge and the foundation pile are already near the yield strength of the steel during the maximum tensile load (section 5.7.9). This load cannot be transferred by a line load. The line area is a fraction of the total surface area. The contact stresses will therefore be much larger than the yield strength. By local yielding the high contact stresses are divided over a larger area and finally over (almost) the whole contact area.

### 5.3 Design loads for ULS and FLS

For the ultimate limit state of the screw thread connection four possible load cases are given based on a typical North Sea offshore wind jacket design by a contractor from the offshore wind industry. In each of the load cases another load condition is dominant. The possible load cases are shown in table 6.

Load condition	Axial Force (kN)	Shear Force (kN)	Bending Moment (kNm)

Table 6 - The four design load cases for the wedge connection in a jacket leg

The screw thread connection is a moment resistant connection. This is the reason that not only tension and compression forces play a role in the load cases but also the bending moment. The

normal stress from the bending moment has to be added to the axial tension or compression. A stress calculation is done for the 2438.4 mm (96 inch) diameter pile with a wall thickness of 50.8 mm (2 inches). This calculation is elaborated below.

First of all some properties of the cross section of the foundation pile are calculated. The area, moment of inertia and second moment of inertia from the foundation pile are calculated here:

$$A_{pile} = \pi * D_{pile} * d_{pile} \rightarrow A_{pile} = \pi * 2387.6 * 50.8 = 3.81 * 10^5 \text{ mm}^2$$

$$I_{pile} = \pi * D_{pile}^3 * d_{pile} \rightarrow I_{pile} = \pi * 2387.6^3 * 50.8 = 2.72 * 10^{11} \text{ mm}^4$$

$$W_{pile} = \frac{I_{pile}}{D_{pile}/2} \rightarrow W_{pile} = \frac{2.72 * 10^{11}}{2438.4/2} = 2.22 * 10^8 \text{ mm}^3$$

The maximum bending and compression stresses are given by:

$$\sigma_{c,pile} = \frac{F_{axial}}{A_{pile}} + \frac{M_{Ed,pile}}{W_{pile}} \rightarrow \sigma_{c,pile} = -\frac{30.6 * 10^6}{3.81 * 10^5} - \frac{6445 * 10^6}{2.22 * 10^8} = -109.3 \text{ MPa}$$

For other diameters the stress follows from the same calculation. The stresses will be higher in smaller pile diameters due a smaller area and a much smaller moment of inertia. The piles which are applied in the offshore wind industry are generally measured in inches. Standard dimensions for diameters of offshore jacket foundation piles are 1.83, 2.14 and 2.44 meter (72, 84 and 96 inches). The results of the maximum tensile and compressive stress for each of these foundation pile diameters with a wall thickness of 50.8 millimeter are given in table 7.

Outer diameter pile	Compressive stress (N/mm <sup>2</sup> )	Tension stress (N/mm <sup>2</sup> )
1828.8 mm (72 inches)		
2133.6 mm (84 inches)		
2438.4 mm (96 inches)		

Table 7 - The maximum axial stress in tension/compression for the different diameters of the foundation pile

#### Fatigue design loads

The fatigue design load cases are not supplied from a contractor from the offshore wind industry. Therefore the damage equivalent load is roughly estimated from the fatigue loads in the monopile - transition piece connection. The damage equivalent load for the wedge connection in the jacket structure is assumed to be one fifth of the ULS-load for xxx million cycles with a lifetime of the jacket structure of 25 years.

## 5.4 Reduction of tolerances

The accuracy tolerances for the installation of the piles are too large to make the screw thread connection successful. Therefore the installation tolerances are reduced. The 'new' tolerances and other properties of the foundation pile for the screw thread connection are given in table 8. In addition to the reduced tolerances the diameter of the foundation pile is also decreased in order to reduce the gap between the jacket leg (connector) and the foundation pile (figure 40).

	New situation	Initial case

Table 8 - Properties and tolerances of the foundation pile in the current and new situation

The rotational tolerance of the foundation pile creates a gap between the foundation pile and the jacket leg. The maximum thickness of this gap is the same as the maximum vertical difference in vertical position of the holes in the foundation pile because all the holes are located at an equal distance from the pile top. The maximum difference in height of the holes between the left and right side of the foundation pile is:

$$\Delta h_{l-r} = \tan(\vartheta_{pile}) * D_{pile} \rightarrow \Delta h_{l-r} = \tan(xx) * 25.4$$

\* xxx = xxx mm

The 10 mm difference between the left and the right side of the holes in the foundation pile is an enormous reduction compared to the 36 mm in the initial situation.

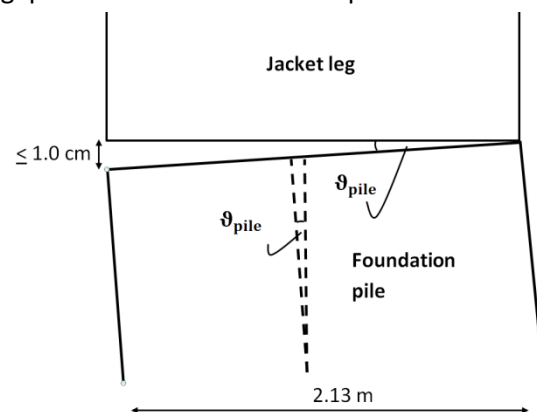


Figure 33 - Height difference between jacket leg and foundation pile

## 5.5 Screw thread

Screw thread is a mechanism to get a vertical movement by the rotation of a member. Screw thread is used as a connection between two parts or for a displacement. Different types of screw threads are available and they have different functions. One of the most known applications of screw thread is the bolt and nut. The screw thread of the bolt is called external screw thread and the thread of the nut is called internal screw thread. Different types of external screw threads are summarized here:

Metric screw thread: Metric screw thread is used in bolts and nuts. The threads have to withstand large forces and are designed in bolts to deform plastically in order to transfer the force from the bolt by multiple threads to the nut. The metric screw thread is available up to diameters of 1000 mm for other applications (Engineers Edge, 2000).

Trapezoidal screw thread: Trapezoidal screw thread has a thread angle of 30 degrees. The thread is generally used for the displacement of a material and not used in connections to transfer large forces.

Square thread: Square thread can be used when low friction is required. The square thread has the lowest friction. The thread is however difficult to manufacture and therefore not applicable with very strict tolerances. For the jacket leg connection, it will be already challenging to make any screw thread with strict tolerances. So this thread is not well suited.

Round thread: The round thread has a high resistance and is therefore not appropriate for this connection.

Buttress thread: This thread is applied when high forces are acting in one direction, so in tension or in compression. The contact surface which takes the force is horizontal and because the other side of the thread is inclined, the thread has a high resistance against bending. In the jacket leg connection the direction of the force changes due to a varying direction of the wind. Therefore, this screw thread is not suitable for the jacket leg connection.

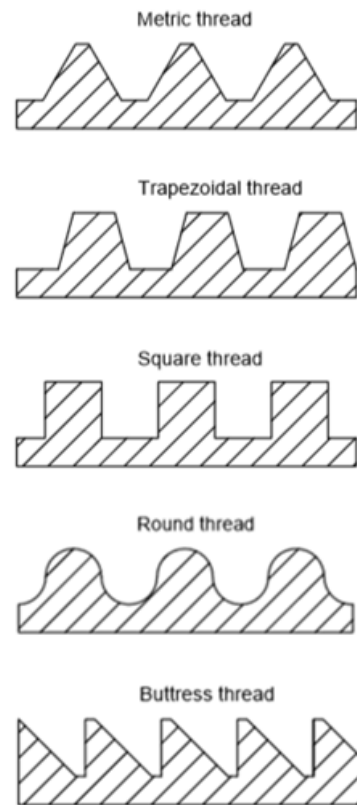


Figure 34 - Different screw thread profiles

## 5.6 Epoxy resin for void between the connector and the pile

	Pure resin	Reinforced-resin

Table 9 - Properties of reinforced- and unreinforced resin

Figure 35 - Locations of the epoxy resin

## 5.7 Other structural components

In this paragraph the several sections in the ultimate limit state are checked.

### 5.7.1 Wedges

The assumption is made that the wedge connection can be modeled as a pinned connection. According to Eurocode 1993-1-8 the wedges have to be checked on shear and bending moment in combination and separately. In the Eurocode the

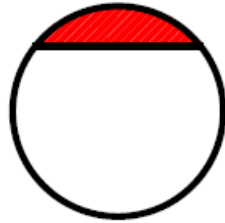


Figure 36 - Cross-section of the wedge at the location of the maximum bending moment

dowel is a round cylinder while the wedge in this thesis is not perfectly round. The red area in figure 47 can be subtracted from the full circle to get the shape of the wedge in the required cross-section. Compared to the Eurocode calculation a reduction for the shear area is needed, a reduction for the bending resistance has to be applied as well.

The shear area of the wedge is 0.81 (Appendix E) times the area of the full circle. This gives a reduction factor of 0.81. The bending resistance in the middle of the wedge is 0.715 (Appendix E) times the bending resistance of a circular cross-section.

So the area of the cross-section of the wedge is given by:

$$A_{wedge} = 0.81 * \frac{1}{4} * \pi * D_{wedge}^2 = 0.81 * \frac{1}{4} * \pi * 100^2 = 6.39 * 10^3 \text{ mm}^2$$

The maximum shear resistance is:

$$F_{v,Rd} = 0.6 * A_{wedge} * \frac{f_u}{\gamma_{m2}} \rightarrow F_{v,Rd} = 0.6 * 6.39 * 10^3 * \frac{550}{1.25} = 1.7 \text{ MN}$$

For one wedge with two shear planes this results in a shear resistance of  $2 * 1.70 = 3.40 \text{ MN}$ . The shear resistance of the whole screw thread connection is  $81.0 \text{ MN}$ .

The maximum bending moment in one wedge is equal to:

$$M_{Ed,wedge} = \frac{F_{Ed,tension}}{8} * (b + 4 * c + 2 * a) \rightarrow M_{Ed,wedge} = \frac{1.22 * 10^5}{8} * (50.8 + 4 * 4.6 + 2 * 30) = 19.7 \text{ kNm}$$

The bending resistance of the wedge with a reduction factor of 0.715 is:

$$W_{el} = \frac{\pi * d^3}{32} \rightarrow W_{el} = 0.715 * \frac{\pi * 100^3}{32} = 7.016 * 10^4 \text{ mm}^3$$

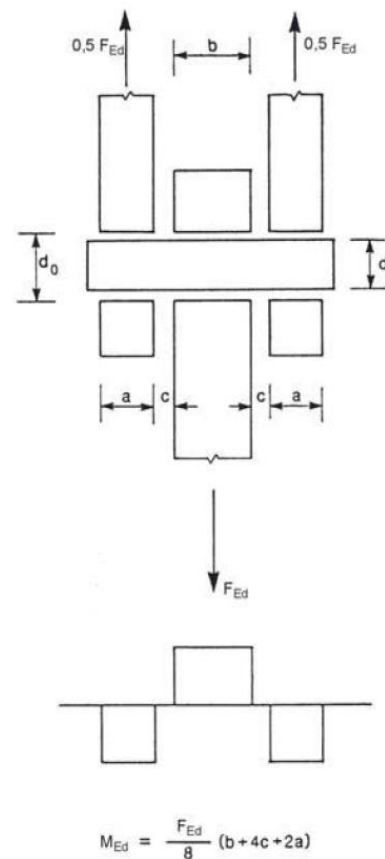


Figure 37 - Bending moment in a dowel according to figure 3.11 from Eurocode 1993-1-8

The maximum allowable bending moment in the wedge at the middle of the foundation pile is:

$$M_{Rd,wedge} = 1.5 * W_{el} * \frac{f_y}{\gamma_{m0}} \rightarrow M_{Rd,wedge} = 1.5 * 7.016 * 10^4 * \frac{460}{1.0} = 48.4 \text{ kNm}$$

The maximum stress in the wedges due to bending is equal to:

$$\sigma_{wedge,max} = \frac{M_{Ed,wedge}}{W_{el}} \rightarrow \sigma_{wedge,max} = \frac{19.7 * 10^6}{7.016 * 10^4} = 280.7 \text{ MPa}$$

The unity check are for bending is:

$$u. c. bending = \frac{M_{Ed,wedge}}{M_{Rd,wedge}} \rightarrow u. c. bending = \frac{19.7}{48.4} = 0.41$$

The unity check for shear is:

$$u. c. shear = \frac{F_{v,Ed}}{F_{v,Rd}} \rightarrow \frac{29.3 * 10^6}{81.0 * 10^6} = 0.36$$

The unity check for the combined shear and bending resistance of the wedge is given by the following formula:

$$\left[ \frac{M_{Ed,wedge}}{M_{Rd,wedge}} \right]^2 + \left[ \frac{F_{v,Ed}}{F_{v,Rd}} \right]^2 \leq 1.0 \rightarrow \left[ \frac{19.7}{48.4} \right]^2 + \left[ \frac{27.6}{60} \right]^2 = 0.50 \leq 1.0$$

All the unity checks are lower than 1.0, the wedges will resist the maximum tensile load.

### 5.7.2 Difference in force on outer flange and inner flange

The force applied at the wedge connection can be assumed to be distributed equally over the area of the wedge connection. The cross-sectional area of the inner flange is smaller than the cross-sectional area of the outer flange of the connector. As a result more force is taken by the outer flange than by the inner flange of the connector. The cross-sectional areas of the inner and outer flange of the connector are respectively:

$$A_{in,fl} = \frac{1}{4} * \pi * (D_{in,con} + 2 * d_{fl,con})^2 - \frac{1}{4} * \pi * D_{in,con}^2 = 1.88 * 10^5 \text{ mm}^2$$

$$A_{out,fl} = \frac{1}{4} * \pi * D_{out,con}^2 - \frac{1}{4} * \pi * (D_{out,con} - 2 * d_{fl,con})^2 = 2.05 * 10^5 \text{ mm}^2$$

$$A_{flanges} = A_{out,fl} + A_{in,fl} = 3.9 * 10^5 \text{ mm}^2$$

The ratio of the inner cross-sectional area and outer cross-sectional area divided by the whole cross-sectional area are respectively:

$$r_{in} = \frac{A_{in,fl}}{A_{flanges}} = 0.478, r_{out} = \frac{A_{out,fl}}{A_{flanges}} = 0.522, r_{out/in} = 1.09$$

The ratio of the outer cross-sectional area divided by the cross-sectional area of the inner flange is:

$$r_{out/in} = \frac{r_{out}}{r_{in}} = 1.09$$

So the cross-section of the outer flange has 9 percent more area than the cross-section of the inner flange and is therefore assumed to take 9 percent more load than the inner flange.

### 5.7.3 Difference in bending moment due to asymmetry

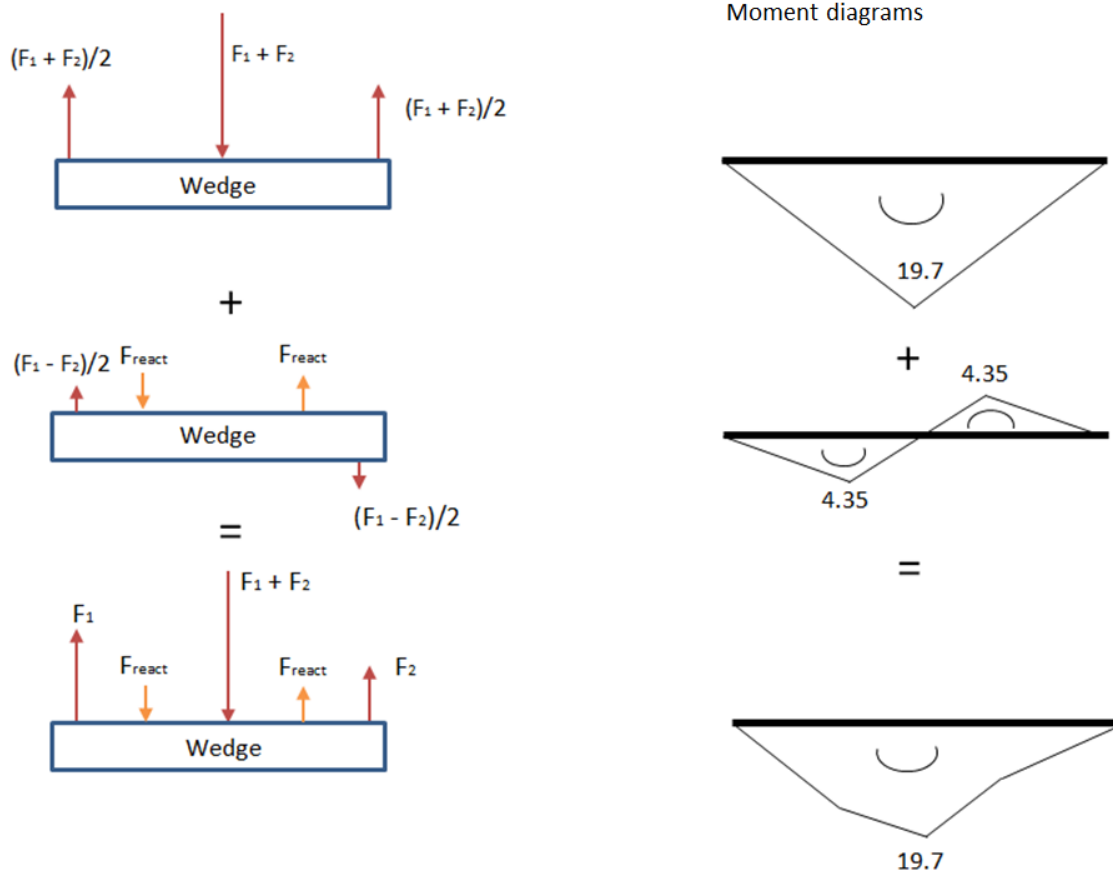


Figure 38 - Forces on the wedge and the corresponding moment diagrams

In case of an equivalent stress over the whole cross-section there will be a larger force acting at the outer flange of the connector than at the inner flange. This introduces a bending moment which is schematic represented in figure 49. In figure 49 (left) the wedges with the forces are presented when the connection is loaded in tension. In figure 49 (right) the corresponding bending moment diagrams are shown. The force  $F_1$  is the force acting from the outer flange to the wedge. The force  $F_2$  is the force applied to the wedge from the inner flange of the connector. The force  $F_1 + F_2$  is the reaction force in the foundation pile. The maximum bending moment in the wedges is 19.7 kNm which occurs in the middle of the wedge due to the force  $(F_1 + F_2)/2$ . Due to the asymmetry of the connection reaction forces will develop in the edges of the foundation pile. These are orange colored in figure 49 and have a value of  $(F_1 - F_2)/2$ . Although the component  $(F_1 - F_2)/2$  has a contribution to the bending moment diagram of the wedge, the maximum bending moment in the middle of the wedge stays the same. So the conclusion is that the location and the value of the maximum bending moment do not change despite the asymmetry between the inner and outer flange of the connector.

### 5.7.4 Compression stress in net area of the foundation pile

The net compression stress in the foundation pile is given by the maximum compression load applied to the connection divided by the net area of the foundation pile. The maximum compression stress between the holes in the foundation pile is:

$$\begin{aligned}\sigma_{c,net,pile} &= \frac{F_{Ed,comp}}{A_{net,pile}} = \frac{F_{Ed,comp}}{A_{pile} - N_{wedge} * D_{wedge} * d_{pile}} \rightarrow \sigma_{c,net,pile} \\ &= \frac{43.3 * 10^6}{\left(\frac{1}{4} * \pi * 2133.6^2 - \frac{1}{4} * \pi * 2032^2\right) - 24 * 50.8 * 100} = 205.7 \text{ MPa}\end{aligned}$$

This is far below the yield strength of the net section of the foundation pile.

### 5.7.5 Tensile stress in net area of the foundation pile

The net tensile stress in the foundation pile is given by the maximum tensile load applied to the connection divided by the net area of the foundation pile. The maximum tensile stress between the holes in the foundation pile is:

$$\begin{aligned}\sigma_{t,net,pile} &= \frac{F_{Ed,comp}}{A_{net,pile}} = \frac{F_{Ed,comp}}{A_{pile} - N_{wedge} * D_{wedge} * d_{pile}} \rightarrow \sigma_{t,net,pile} \\ &= \frac{29.3 * 10^6}{\left(\frac{1}{4} * \pi * 2133.6^2 - \frac{1}{4} * \pi * 2032^2\right) - 24 * 50.8 * 100} = 139.2 \text{ MPa}\end{aligned}$$

This is far below the yield strength of the net section of the foundation pile.

### 5.7.6 Additional stress due to bending moment in the foundation pile

In section 5.5.2 the assumption is made that the stress in the inner and outer flange of the connector is equal. The cross-sectional area of the inner flange is smaller than the cross-sectional area of the outer flange. When the connection is loaded by tensile loading this will result in a bending moment in the foundation pile. This results in additional tensile stress at the outer side of the foundation pile. The additional bending moment per wedge in the foundation pile due to the tensile load is equal to:

$$\begin{aligned}M_{circ,con} &= (A_{out,fl} * a_{out,fl} - A_{in,fl} * a_{in,fl}) * \sigma_{t,con} / N_{wedges} \rightarrow M_{circ,con} \\ &= (205 * 10^3 * 45 - 188 * 10^3 * 45) * 75 / 24 = 2.4 \text{ kNm/wedge}\end{aligned}$$

The additional stress in net section of the foundation pile due to the bending moment is equal to:

$$\sigma_{t,add,net,pile} = \frac{M_{circ,con} * \frac{d_{pile}}{2}}{\frac{1}{12} * b_{net,seg} * d_{pile}^3} \rightarrow \sigma_{t,add,net,pile} = \frac{2.4 * 10^6 * \frac{50.8}{2}}{\frac{1}{12} * 179.3 * 50.8^3} = 31.1 \text{ MPa}$$

The total tension stress at the outer side of the net section of the foundation pile is equal to:

$$\sigma_{t,net,pile} = \sigma_{t,net,pile} + \sigma_{t,add,net,pile} \rightarrow \sigma_{t,net,pile} = 139.2 + 31.1 = 170.3 \text{ MPa}$$

This is far below the yield strength of the foundation pile, so this is okay.

### 5.7.7 Tensile stress in net area of the connector

The tension in the net area of the connector is calculated on the same way as the tension in the net section of the foundation pile. Compressive stresses in the net area of the connector are not possible because when the connection is loaded in compression; all the compressive stresses are directly transferred by the contact plane between the connector and the foundation pile. Assuming that the stress in both flanges is the same, the maximum stress is obtained in the net section of the inner flange. The maximum tensile stress in the net area of the inner flange of the connector is:

$$\sigma_{t,net,con} = \frac{r_{in} * F_{Ed,tension}}{A_{flanges} - N_{wedges} * D_{wedge} * d_{fl,con}} \rightarrow \sigma_{t,net,con} = \frac{0.478 * 29.3 * 10^6}{1.88 * 10^5 - 24 * 100 * 30} = 120.7 \text{ MPa}$$

The stress in the net area of the connector stays far below the yield strength and the net section of the connector meets its requirements.

### 5.7.8 Contact stress between wedge and connector

The contact stress between the wedges and the connector is investigated at the outer flange. The outer flange transfers 52.2 percent of the load during the maximum tensile loading. So the contact stress in the between the outer flange of the connector and the foundation pile is higher than the contact stress between the inner flange of the connector and the wedge. The force transferred by the outer flange is  $0.522 * 29.3 * 10^6 = 15.3 * 10^6 \text{ N}$ . The contact stress between the wedge and the foundation pile is given by:

$$\sigma_{con,wedge} = \frac{r_{out} * F_{Ed,tension}}{A_{con,wedge} * N_{wedges}} \rightarrow \sigma_{conn,wedge} = \frac{15.3 * 10^6}{30 * 100 * 24} = 212 \text{ Mpa}$$

This is far below the yield strength of the connector and the wedge, so the wedge and the connector fulfill their requirements.

### 5.7.9 Contact stress between wedge and foundation pile

The contact stress between the wedge and the foundation pile will be larger than the contact stress between the wedges and the connector. Firstly, the thickness of the foundation pile is less than the combined thickness of the two flanges of the connector. Secondly, the contact area between the wedge and the foundation pile is reduced due to the shape of the wedge (figure 50). The contact area between the wedge and the foundation pile is at its minimum when the wedge is pushed as far as possible into the connection.

*Figure 39 - Cross-sectional view of the wedge at the contact area (left) and the minimum contact area between wedge and foundation pile (right)*

To calculate the contact stress between the wedge and the foundation pile, the minimum contact area between the wedge and the foundation pile has to be determined. This is done by using figure 50. At the origin of the x-axis the wedge starts to have a negative inclination  $\alpha$ . With this information and figure 50 the following geometrical dimensions can be calculated:

$$a(x) = \tan(\alpha) * x, \quad \beta(x) = \arcsin\left(\frac{R_{wedge} - a(x)}{R_{wedge}}\right), \quad L(x) = \cos(\beta(x)) * R_{wedge}$$

The contact area is calculated by taking the integral of  $2 * L(x)$  in which  $gap + 20$  is the lower bound and  $gap + 20 + d_{pile}$  is the upper bound. The contact area between the wedge and the foundation pile is given as:

$$A_{cont,wedge,pile} = \int_{gap+20}^{gap+20+d_{pile}} 2 * L(x) dx$$

By substitution all the geometrical dimensions defined above in the equation of the contact area between the wedge and the foundation pile gives the following expression:

$$A_{cont,wedge,pile} = \int_{gap+20}^{gap+20+d_{pile}} 2 * \cos\left(\arcsin\left(\frac{D_{wedge} - \tan(\alpha) * x}{D_{wedge}}\right)\right) * D_{wedge} dx$$

By calculating this integral the contact area between the wedge and the foundation pile is  $0.56 *$  the contact area taken for a circular wedge. This is the red area of the total colored area in figure 50.

Now the contact stress between the wedge and the foundation pile is determined as follows:

$$\sigma_{cont,pile,wedge} = \frac{F_{Ed,tension}}{A_{cont,wedge,pile} * N_{wedges}} \rightarrow \sigma_{cont,pile,wedge} = \frac{29.3 * 10^6}{0.56 * 50.8 * 100 * 24} = 429 \text{ MPa}$$

The maximum allowable contact stress is the yield strength of the material. This is  $460 \text{ N/mm}^2$ . The  $\sigma_{cont,pile,wedge}$  is close to the yield strength, but this section meets still the requirements for the tensile load in the ultimate limit state.

### 5.7.10 Actuation force

The maximum compression pressure which can be delivered by the actuators is assumed to be 800 bar to limit the costs of the actuators. This is 80 MPa. So the maximum actuation force per wedge with a diameter of 100 millimeter is:

$$F_{actuator} = p_{actuator} * A_{wedge} = p_{actuator} * \frac{1}{4} * \pi * D_{wedge}^2 \rightarrow F_{actuator} = 80 * \frac{1}{4} * \pi * 100^2 = 628 \text{ kN}$$

In case of full preloading, the preload in the connection have to be minimum the tensile load in the ULS. The maximum tension per wedge in the ULS is equal to:

$$29.3 * \frac{10^6}{24} = 1.22 \text{ MN/wedge}$$

The horizontal actuation force will create a vertical preload in the wedge connection due to the inclination of the wedge. In addition the horizontal actuation force will create friction between

the wedge and the foundation pile and connector (figure 51). This results in the following calculation (figure 51):

$$F_{hor,pre} = \frac{(\tan(\alpha) * F_{Ed,tension})}{N_{wedges}} \rightarrow F_{hor,pre} = \frac{\tan(10) * 29.3 * 10^6}{24} = 215 \text{ kN}$$

The friction coefficient  $\mu$  of the wedge is assumed to be 0.15. The friction load is calculated as follows:

$$F_{fr,wedge} = 2 * \frac{F_{Ed,tension} * \mu}{N_{wedges}} + 2 * \frac{F_{Ed,tension} * \mu^2 * \tan(\alpha)}{N_{wedges}} \text{ (second order)}$$

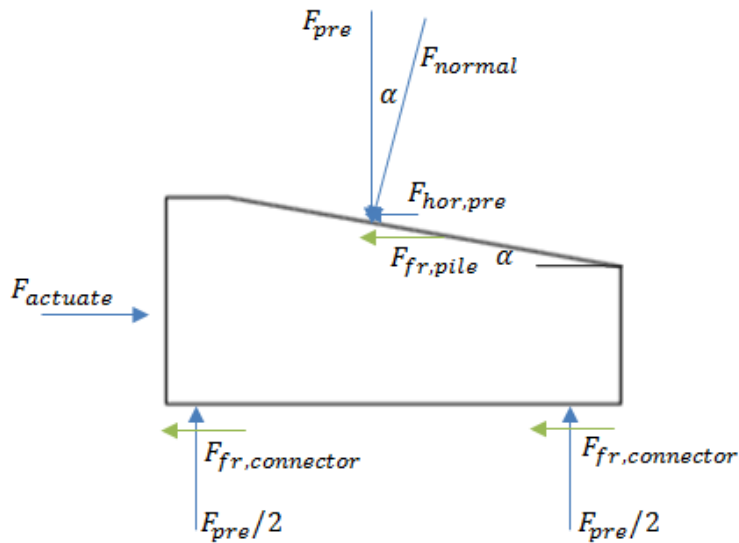
$$\rightarrow F_{friction,wedge} = 2 * \frac{29.3 * 10^6 * 0.15}{24} + 2 * \frac{29.3 * 10^6 * 0.15^2 * \tan(10)}{24}$$

$$= 376 \text{ kN}$$

The total actuation force per wedge is equal to:

$$F_{actuate} = F_{hor,pre} + F_{fr,wedge} \rightarrow F_{actuate} = 215 + 376 = 591 \text{ kN}$$

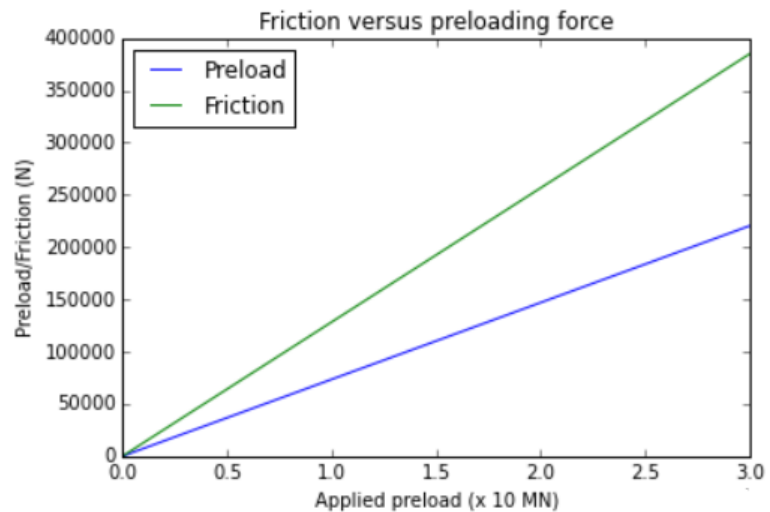
This is smaller than the maximum preload which can be applied by the actuator when a maximum of 800 bar is allowed.



### 5.7.11 Self-locking system

After the installation of the wedges the force  $F_{hor,pre}$  pushes the wedge to the outside of the connection. Friction forces will develop in the opposite direction, so to the inside of the

connection. When the friction force is larger than the horizontal component of the preload or tension, the wedge will remain in the connection without any external pressure. In figure 52 the friction force is plotted for  $\mu = 0.15$  and the preload is plotted for an inclination of the wedge of 10 degrees. As can be seen in this figure the friction force is always larger than the horizontal component of the preloading force. In case of deterioration of the contact surface between the wedges and the foundation pile, the friction force is still large enough to compensate the outward force. The frictional force is still larger than the horizontal component of the preloading force for  $\mu = 0.09$ . So no constrain for the wedge at the outer flange is required.



### 5.7.12 Distance from the central axis of the wedge to the edge of the flange

The distance from the central axis of the wedge to the edge of the flange is colored red in figure 53 as well as the distance from the central axis of the wedge to the edge of the foundation pile. These sections have only to be calculated for a tensile force in the jacket leg, because the compression force is directly taken by the surface between the connector and the foundation pile. The maximum tensile load is 29.3 MN. This is divided by the two flanges of the connector. The outer flange of the connector gets 15.3 MN. This is 0.64 MN per wedge. To calculate the distance from the central axis of the wedge to the bottom of the outer flange the formulas for the bolts in Eurocode 1993-1-8 table 3.4 is used.

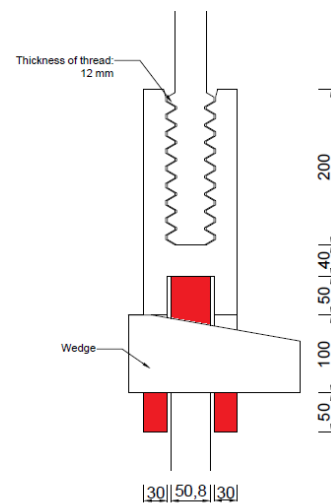


Figure 41 - Outer flange

Bearing resistance <sup>a,b,c,d</sup>	$F_{b,Rd} = \frac{k_1 \alpha_b f_u d t}{\gamma_{M2}}$
	where $\alpha_b$ is the smallest of $\alpha_d$ ; $\frac{f_{ub}}{f_u}$ or 1,0;
	in the direction of load transfer:
	— for end bolts: $\alpha_d = \frac{e_1}{3a_0}$ ; for inner bolts: $\alpha_d = \frac{p_1}{3a_0} - \frac{1}{4}$
	perpendicular to the direction of load transfer:
	— for edge bolts: $k_1$ is the smallest of 2,8 $\frac{e_2}{d_0} - 1,7$ , 1,4 $\frac{p_2}{d_0} - 1,7$ and 2,5
	— for inner bolts: $k_1$ is the smallest of 1,4 $\frac{p_2}{d_0} - 1,7$ and 2,5

Table 10 - Part of table 3.4 of Eurocode 1993-1-8

According to Eurocode 1993-1-8 table 3.4 the bearing resistance of the outer flange is:

$$F_{b,Rd} = \frac{k_1 * \alpha_b * f_u * D_{wedge} * d_{flange}}{\gamma_{m2}} \rightarrow \frac{2.11 * 0.33 * 550 * 100 * 30}{1.25} = 0.94 \text{ MN}$$

With:

$$k_1 = \min\left(2.8 * \frac{e_2}{d_0} - 1.7, 1.4 * \frac{p_2}{d_0} - 1.7, 2.5\right) = 2.11$$

$$\alpha_b = \min\left(\frac{e_1}{3 * d_0}, \frac{f_{uw}}{f_u}, 1.0\right) = 0.33$$

This gives a unity check of:

$$u. c. b, flange = \frac{F_{b,Ed}}{F_{b,Rd}} = \frac{0.64}{0.94} = 0.68$$

Applying the same formulas to the holes in the foundation pile gives a unity check of:

$$u. c. b, pile = \frac{F_{Ed, tension} / N_{wedges}}{F_{b,Rd, pile}} = \frac{1.22}{1.58} = 0.77$$

So there is enough space around the holes in the connector and in the foundation pile.

## 5.6 The actuation force on the connector

In this paragraph is looked for the best option to install the wedges. The wedges can be installed all simultaneously or in groups to determine of the outer flanges of the connector has to be stiffened. To check this out two FEM-models are built.

The software package ANSYS Workbench is used to calculate the models. The geometry of the models is drawn in the software package Solid Edge and is imported to ANSYS Workbench. In Solid Edge all the components of the connection are drawn separately. In ANSYS Workbench all the contact areas between the several components have to be defined. All the contact surfaces are frictional with a frictional coefficient of 0.15. Only the upper 500 millimeters of the foundation pile is modeled. The bottom surface of the foundation pile is fixed. Furthermore no supports are applied.

For all the structural components structural steel is used with a young's modulus of 210 GPa. The mesh is done automatically by ANSYS Workbench and a mesh with medium tetrahedral elements is obtained. This is good enough for a first indication for the locations of the maximum stresses.

In the first model the wedges are installed in groups of four. One fourth of the screw thread connection is modeled and the by using the cyclic symmetry option the whole geometry is defined. A little bit of the actuator is modeled (figure 54) to apply the reaction force at that surface. The actuation load of 591 kN is applied to one wedge and the reaction force of 591 kN is applied to the actuator.

*Figure 42 - Cyclic symmetry with boundary conditions of first model*

In figures 55 to 57 the results of the FEM-calculation are shown. From figure 55 and 57 can be seen that the principle stress occurs below the actuator. Only below the actuator the maximum principle stress exceeds the yield stress. The maximum principle stress is around 400 MPa at the location which was assumed to be critical. From and bottom view (figure 56) can be seen that the ring stiffness is quite strong and the actuation force is transferred more by the ring stiffness than by the bending stiffness.

*Figure 43 - Principle stress in the outside of the connection*

In the second FEM-model all the wedges are installed simultaneously. 1 of the 24 segments is modeled and a cyclic symmetry is used. By using the cyclic symmetry the whole geometry is defined. The actuation force of 591 kN is applied to all the wedges and the reaction force of 591 kN is applied to all the actuators.

*Figure 45 - Maximum principle stress in the cross-section of the wedge connection*

*Figure 44 - Deformation of the flange during the installation of the wedge*

In figure 58 the maximum principle stress around the connection are shown. The location of the maximum principle stress is below the actuators. That is the only location where the principle stresses exceed the yield strength. From the maximum principle stress around the wedges and the deformation of the outer flange below the wedges (figure 59) can be concluded that the ring stiffness takes a big part of the load. The maximum principle stress at the compared location is a little bit above 400 MPa. This is comparable to the result of the first model.

*Figure 46 - Maximum principle stresses at the outer flange*

*Figure 47 - Total deformation of the outer flange of the connection*

*Figure 48 - Maximum principle stress at the desired location*

From the two analyzes the conclusion can be drawn that the wedges can better be installed simultaneously because the ring flange stiffness of the connector takes the biggest part of the load. The ring flange stiffness can only be utilized by a load which is distributed along the whole

ring flange. By installing more wedges simultaneously the load is more equally distributed along the flange and the stiffness of the ring flange is utilized more. However, this connection does not necessarily have to be preloaded and therefore the outer flange of the connector does not necessarily have to be stiffened. In case of preloading the screw thread connection, the outer flanges of the connector have to be stiffened.

Local shear stress around the actuator in the outer flange

In section 5.7.10 is calculated that the maximum required force from the actuators per wedge is 591 kN . This is intercepted by the outer flange of the connector. To calculate the shear stress in the outer flange of the connector it is assumed that the diameter of the actuator is 100 mm + 2\*10 = 120 millimeter. So the area of the shear force is:

$$\pi * (D_{wedge} + t_{actuator} * 2) * d_{flange} = \pi * (100 + 20) * 30 = 11309 \text{ mm}^2$$

This gives a maximum shear stress of:

$$\tau_{con} = \frac{591 * 10^3}{11309} = 52.2 \text{ MPa}$$

This is clearly below the maximum allowable shear stress, so the outer flange can resist the local introduced force from the actuators.

**5.7 Results for the ultimate limit state**

The results of the most important ULS-sections are summarized in the table 12.


Table 11 - Unity checks in ULS for the screw thread connection

Figure 49 - Unity checks for the ultimate limit state

For the ultimate limit state all the sections suffices the requirements.

**5.8 Fatigue limit state for screw thread connection**

Fatigue occurs due to repetitive cyclic loading. Discontinuities in the geometry of the connection contribute to larger cyclic stresses. Hence the discontinuities require special attention for fatigue. For this concept special attention to fatigue should be paid to the holes for the wedges or near the screw thread. Another section which can be checked is the bottom of the wedge

which is loaded in tension. The four sections are checked by a hand calculation according to Eurocode 1993-1-9. The connection is checked without preload, if the damage stays below 1.0, the connection will suffice also the requirements for fatigue in case of a preloaded the connection. As shown in figure 62 the critical sections on fatigue are numbered. Number 1 is the bottom of the wedge. The fatigue calculation for this part is done in section 5.8.1. Number 2 are the locations next to the holes of the foundation piles. The fatigue calculation for this part is done in section 5.8.2. The holes next to the connector are determined as number 3 and calculated on fatigue in section 5.8.3. Number 4 is the screw thread and the fatigue of the screw thread is calculated in section 5.8.4.

### 5.8.1 Fatigue in the wedges

Only when the screw thread connection is loaded with a tensile load, a bending moment is introduced to the wedges. Since fatigue occurs more easily in tension than in compression, a fatigue failure will occur in the bottom of the wedge. The surface of the outer wedge is very smooth. Therefore is the fatigue detail category the highest possible category. However, this category is used for pure axial stress. So a reduction of 10 percent is applied to the detail category. With the 10 percent reduction the bottom of the wedge is detail category 144.

Detail category	Constructional detail	Description	Requirements
160	<p>NOTE The fatigue strength curve associated with category 160 is the highest. No detail can reach a better fatigue strength at any number of cycles.</p>	<p>Rolled and extruded products:</p> <ol style="list-style-type: none"> <li>1) Plates and flats;</li> <li>2) Rolled sections;</li> <li>3) Seamless hollow sections, either rectangular or circular.</li> </ol>	<p>Details 1) to 3):</p> <p>Sharp edges, surface and rolling flaws to be improved by grinding until removed and smooth transition achieved.</p>

Figure 51 - Detail category on fatigue according to Eurocode 1993-1-9

The tensile stress in the bottom of the wedge is 280.7 MPa. So the damage equivalent load is  $280.7 / 5 = 56.1$  MPa for 10 million cycles. Starting with 2 million cycles with a stress range of 144 MPa, gives in the SN-curve a value in for 5 million cycles of:

$$\Delta\sigma_R^m * N_R = \Delta\sigma_C^m * 2 * 10^6 \rightarrow \Delta\sigma_R^m = \Delta\sigma_C^m * \frac{2 * 10^6}{N_R} \rightarrow \Delta\sigma_R^m = 144 * \left(\frac{2 * 10^6}{5 * 10^6}\right)^{\frac{1}{3}} = 106.1$$

For 10 million cycles the SN-curve of detail category 144 has a value of:

$$\Delta\sigma_R^m * N_R = \Delta\sigma_C^m * 2 * 10^6 \rightarrow \Delta\sigma_R^m = \Delta\sigma_C^m * \frac{5 * 10^6}{N_R} \rightarrow \Delta\sigma_R^m = 106.1 * \left(\frac{5 * 10^6}{1 * 10^7}\right)^{\frac{1}{5}} = 92.4$$

Therefore the maximum allowable number of cycles for a tensile stress of 56.1 MPa at the bottom of the wedge is equal to:

$$\begin{aligned} \Delta\sigma_R^m * N_R &= \Delta\sigma_C^m * 1 * 10^7 \rightarrow N_R = \frac{\Delta\sigma_C^m}{\Delta\sigma_R^m} * 1 * 10^7 \rightarrow N_R = \left(\frac{92.4}{1.35 * 56.1}\right)^3 * 1 * 10^7 \\ &= 1.53 * 10^7 \text{ cycles} \end{aligned}$$

By applying Minor's rule the damage in the wedge is:

$$D = \sum_{i=1}^N \frac{n_i}{N_i} \leq 1.0 \rightarrow D = \frac{1 * 10^7}{1.53 * 10^7} = 0.66 < 1.0$$

The damage is below 1.0, so the wedges fulfill the requirements on fatigue.

### 5.8.2 Fatigue next to the holes in the foundation pile

To determine the fatigue next to the holes in the foundation pile detail category 11 from figure 64 is used. This has a fatigue detail class of 90. According to Eurocode 1993-1-9 the total force has to be divided by the net area of the foundation pile. The holes in the foundation piles are not completely round. But they will have a nod at the top to make an aligned contact surface between the inclination of the wedge and the foundation pile. This part is not investigated, but a reduction on the detail class is made to compensate for the nod. This reduction is taken as 10 percent of the detail class. So the detail class for this connection is 81.

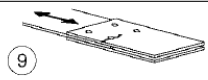
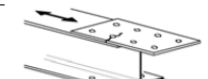
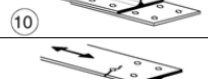
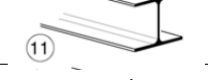
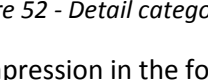
90		bolts. 9) Double covered joint with fitted bolts.	9) ... net cross-section.	$e_1 \geq 1,5 d$
		9) Double covered joint with non preloaded injection bolts.	9) ... net cross-section.	Edge distance: $e_2 \geq 1,5 d$
		10) One sided connection with preloaded high strength bolts.	10) ... gross cross-section.	Spacing: $p_1 \geq 2,5 d$
		10) One sided connection with preloaded injection bolts.	10) ... gross cross-section.	Spacing: $p_2 \geq 2,5 d$
		11) Structural element with holes subject to bending and axial forces	11) ... net cross-section.	Detailing to EN 1993-1-8, Figure 3.1

Figure 52 - Detail category on fatigue according to Eurocode 1993-1-9

The net stress in compression in the foundation pile is  $205.7 \text{ N/mm}^2$  while the tension stress in the net section of the foundation pile is  $170.3 \text{ N/mm}^2$ . According to Eurocode 1993-1-9 only 60 percent of the compression stress has to be taken into account for a fatigue calculation. The net stress in compression for the fatigue calculation is  $123.4 \text{ MPa}$ . So the cyclic loading for the tensile stress is higher and therefore decisive. So the equivalent damage load is  $170.6 / 5 = 34.1 \text{ MPa}$  for 10 million cycles. With the knowledge that the SN-curve has a value of  $81 \text{ MPa}$  for 2 million cycles, the value for 5 million cycles is:

$$\Delta\sigma_R^m * N_R = \Delta\sigma_C^m * 2 * 10^6 \rightarrow \Delta\sigma_R^m = \Delta\sigma_C^m * \frac{2 * 10^6}{N_R} \rightarrow \Delta\sigma_R^m = 81 * \left( \frac{2 * 10^6}{5 * 10^6} \right)^{\frac{1}{3}} = 59.7$$

For 10 million cycles the SN-curve for detail category 81 has a value of:

$$\Delta\sigma_R^m * N_R = \Delta\sigma_C^m * 2 * 10^6 \rightarrow \Delta\sigma_R^m = \Delta\sigma_C^m * \frac{5 * 10^6}{N_R} \rightarrow \Delta\sigma_R^m = 66.3 * \left( \frac{5 * 10^6}{1 * 10^7} \right)^{\frac{1}{5}} = 52.0$$

From here follows that the maximum allowable number of cycles in the net section of the foundation pile is:

$$\begin{aligned} \Delta\sigma_R^m * N_R &= \Delta\sigma_C^m * 1 * 10^7 \rightarrow N_R = \frac{\Delta\sigma_C^m}{\Delta\sigma_R^m} * 1 * 10^7 \rightarrow N_R = \left( \frac{52.0}{1.15 * 34.1} \right)^3 * 1 * 10^7 \\ &= 9.5 * 10^6 \text{ cycles} \end{aligned}$$

By applying Minors Rule the damage in the connection is:

$$D = \sum_{i=1}^N \frac{n_i}{N_i} \leq 1.0 \rightarrow D = \frac{1 * 10^7}{9.5 * 10^6} = 1.05 > 1.0$$

This is a bit higher than 1.0. But because the exact fatigue loads on the screw thread connection are not known, the criterion on fatigue is in this stage sufficient.

### 5.8.3 Fatigue next to the holes of the connector

The holes in the connector are round and only loaded in tension. The net section of the connector is not loaded in compression because the compressive load is directly taken by the contact surface between the connector and the foundation pile. So the flanges of the connector have only to be checked on fatigue in tension. Construction detail 11 in figure 64 represents exactly this situation. The corresponding detail category for construction detail 11 is detail class 90. The maximum tensile stress in the net area of the connector is 120.7 MPa. So the damage equivalent load for the net section of the connector is  $120.7 / 5 = 24.2$  MPa for 10 million cycles. With the knowledge that the SN-curve has a value of 90 MPa for 2 million cycles, the value of the SN-curve for 5 million cycles is:

$$\Delta\sigma_R^m * N_R = \Delta\sigma_C^m * 2 * 10^6 \rightarrow \Delta\sigma_R^m = \Delta\sigma_C^m * \frac{2 * 10^6}{N_R} \rightarrow \Delta\sigma_R^m = 90 * \left(\frac{2 * 10^6}{5 * 10^6}\right)^{\frac{1}{3}} = 66.3$$

For 10 million cycles the SN-curve of detail category 90 has a value of:

$$\Delta\sigma_R^m * N_R = \Delta\sigma_C^m * 2 * 10^6 \rightarrow \Delta\sigma_R^m = \Delta\sigma_C^m * \frac{5 * 10^6}{N_R} \rightarrow \Delta\sigma_R^m = 66.3 * \left(\frac{5 * 10^6}{1 * 10^7}\right)^{\frac{1}{5}} = 57.73$$

From here follows that the maximum allowable number of cycles in the net section of the foundation pile is:

$$\begin{aligned} \Delta\sigma_R^m * N_R &= \Delta\sigma_C^m * 1 * 10^7 \rightarrow N_R = \frac{\Delta\sigma_C^m}{\Delta\sigma_R^m} * 1 * 10^7 \rightarrow N_R = \left(\frac{\frac{57.73}{1.15}}{1.35 * 24.2}\right)^3 * 1 * 10^7 \\ &= 3.63 * 10^7 \text{ cycles} \end{aligned}$$

By applying Minors Rule the damage at the end of the lifetime of the connection is:

$$D = \sum_{i=1}^N \frac{n_i}{N_i} \leq 1.0 \rightarrow D = \frac{1 * 10^7}{3.63 * 10^7} = 0.28 < 1.0$$

The damage is much lower than 1.0, so this section will not be vulnerable to fatigue.

### 5.8.3 Fatigue in the screw thread

Screw threads are always sensible to fatigue. In the Eurocode the detail class for the screw threads in bolts is 50. In this situation the screw thread profile is much larger than the screw thread in a bolted connection. To be conservative for a new connection the detail class of the screw thread of this connection is assumed to be 45 instead of 50 (10 percent reduction). The

direction of the loading does not influence the fatigue behavior around the screw thread. So the maximum load in the axial direction is the decisive load in fatigue. This is the compression load with a maximum stress in the jacket leg of 165.1 MPa. So the damage equivalent load is  $165.1 / 5 = 33.0$  MPa. For 2 million cycles the SN-curve has a value of 45. So for 5 million cycles the SN-curve has a value of:

$$\Delta\sigma_R^m * N_R = \Delta\sigma_C^m * 2 * 10^6 \rightarrow \Delta\sigma_R^m = \Delta\sigma_C^m * \frac{2 * 10^6}{N_R} \rightarrow \Delta\sigma_R^m = 45 * \left(\frac{2 * 10^6}{5 * 10^6}\right)^{\frac{1}{3}} = 33.2$$

For 10 million cycles the SN-curve has a value of:

$$\Delta\sigma_R^m * N_R = \Delta\sigma_C^m * 2 * 10^6 \rightarrow \Delta\sigma_R^m = \Delta\sigma_C^m * \frac{5 * 10^6}{N_R} \rightarrow \Delta\sigma_R^m = 33.2 * \left(\frac{5 * 10^6}{1 * 10^7}\right)^{\frac{1}{5}} = 28.9$$

The maximum allowable number of cycles in the screw thread of the wedge connection is therefore:

$$\begin{aligned} \Delta\sigma_R^m * N_R = \Delta\sigma_C^m * 1 * 10^7 \rightarrow N_R = \frac{\Delta\sigma_C^m}{\Delta\sigma_R^m} * 1 * 10^7 \rightarrow N_R &= \left(\frac{\frac{28.9}{1.15}}{1.35 * 33.0}\right)^3 * 1 * 10^7 \\ &= 0.18 * 10^7 \text{ cycles} \end{aligned}$$

By applying Minors Rule the damage in the screw thread is:

$$D = \sum_{i=1}^N \frac{n_i}{N_i} \leq 1.0 \rightarrow D = \frac{1 * 10^7}{1.08 * 10^7} = 5.6 > 1.0$$

The damage in the screw thread is much higher than 1.0, so this is not sufficient. Solutions to reduce the damage are: Thickening of the jacket leg, so that the maximum axial stress can be reduced and by replacing the metric screw thread by the trapezoidal screw thread. In this case the peak stress in the screw thread can be reduced.

## 5.9 Results for the fatigue limit state

The results for the fatigue limit state are summarized in table 13.

Section	Damage
<b>1. Maximum tension stress in the wedges</b>	0.66
<b>2. Nominal stress between holes foundation pile</b>	1.05
<b>3. Nominal stress between holes connector</b>	0.28
<b>4. Maximum tension stress in the screw thread</b>	5.6

Table 12 - Results for the fatigue limit state

For the fatigue limit state can be concluded that the screw thread is the most vulnerable for fatigue.

## 5.10 Closing of the gap between the connector and foundation pile

In this section is checked if the gap between the foundation pile and the connector can be closed by preloading of the wedge connection. In case the foundation pile has its maximum tilt, the maximum thickness of the gap is 10 millimeter. The connector and the foundation pile touch each other only at one location (figure 40). So the gap has a length of almost 360 degrees. This is the perimeter of the foundation pile. The force needed to close a gap (perimeter) between two tubulars is determined by three stiffness's (Seidel, 2018).

- The shell stiffness of the foundation pile
- The shell stiffness of the jacket leg
- The stiffness of the flanges of the connector

For the foundation pile the stiffness is only determined by the shell stiffness of the pile. The shell of the foundation pile is determined as infinitely long (15 meter) and results in axial deformation.

The jacket leg is at two meters from the wedge connection attached to horizontal and diagonal braces. These braces increase the stiffness of the jacket leg. Therefore, the shell stiffness of the infinite long jacket leg is multiplied by two.

So shell stiffness's of the foundation pile and the jacket leg are given as follows (Seidel, 2018):

$$k_{shell,fp} = \frac{E * d_{pile}}{1.8 * l_{gap}}$$

$$k_{shell,jl} = \frac{2 * E * t_{jl}}{1.8 * l_{gap}}$$

The stiffness of the flanges is determined by:

$$k_{flange} = \frac{384 * EI_{flanges}}{l_{gap}^4}$$

With  $I_{flanges} = \frac{1}{12} * 2 * d_{flange} * h_{flange}^3$  and  $l_{gap} = \pi * D_{pile}$

The deformation of the jacket leg consists of the deformation of the shell and the deformation of the flanges of the connector. The deformation of the flanges of the connector and the jacket leg are not the same. Therefore, this is a serial system. In a serial system the deformation of the different components are added to each other. So, the deformation of the shell and the deformation of the flanges have to be added to get the deformation of the jacket leg. The deformation in the foundation pile is only determined by the infinitely long shell.

For a wall thickness of 50.8 mm (2 inch) of the foundation pile, the contact stress between the wedges and the foundation pile is critical. For the tensile load in ULS the unity check for the

contact stress between the wedges and the foundation pile is 0.93. A little additional load can be applied to close the gap in order to stay below the yield strength at the contact surface of the wedge. Therefore by closing the gap between the foundation pile and the jacket leg, the thickness of the foundation pile has to be increased. The possibility of closing the gap is determined here for a wall thickness of 60, 70 and 80 mm. The stiffness of the shell increases linearly by the thickness of the foundation pile, but the contact area between the wedge and the foundation pile increases quadratic.

Fatigue does not occur due to the height of the stress, but due to cyclic loading. Therefore the force which is required to close the gap does not have any influence on the fatigue behaviour of the connection. So the maximum force which can be applied is the maximum tensile force which can be resisted by the connection minus the tensile load in the ULS. The tensile load in the ULS is for a 2.13 meter (84 inch) diameter pile 29.3 MN. Three components of the wedge connection will be checked to determine the maximum additional tensile force they can resist.

The first component is the maximum tensile stress in the wedge. The allowable preload in the wedge will decrease due to an increase of length of the wedge by increasing the pile thickness. And therefore the bending moment of the wedge increases. The second component is the contact stress between the foundation pile and the wedge. The allowable preload for the contact surface will increase due to the increase of the surface between the wedges and the foundation pile by an increasing pile thickness. The third component is the contact stress of the wedges and the connector. The allowable additional force between the wedges and the connector will be equal for all pile thicknesses. Because there is no change between the contact area of the wedges and the connector by increasing the wall thickness of the foundation pile. The maximum applicable preload to close the gap is the component in which the allowable preload is the lowest of all the components (table 14).

<b>Pile thickness (mm)</b>	<b>Preload bending wedge (MN)</b>	<b>Preload contact wedge - pile (MN)</b>	<b>Preload contact wedge - connector (MN)</b>
<b>50.8</b>	16.6	1.55	36.9
<b>60</b>	13.6	7.1	36.9
<b>70</b>	10.9	13.2	36.9
<b>80</b>	8.3	19.3	36.9

*Table 13 - The maximum allowable preload for several components of the wedge connection for different thicknesses of the foundation pile*

By taking for all the different wall thickness's the minimum allowable load in table 14, the maximum allowable preloading forces for the different pile thicknesses are given in table 15. The corresponding closable gap for the maximum allowable tensile load is given. Due to the tolerances in the screw thread, the assumption is made that 2 millimeter of the gap can be closed by closing the tolerances of the screw thread. The maximum closable gap including the closing of the tolerances of the screw thread is also given in table 15.

<b>Pile thickness (mm)</b>	<b>Preloading force (MN)</b>	<b>Maximum closable gap (mm)</b>	<b>Maximum closable gap with tolerance (mm)</b>
----------------------------	------------------------------	----------------------------------	---

<b>50.8</b>	1.55	0.42	2.42
<b>60</b>	7.1	1.76	3.76
<b>70</b>	10.9	2.49	4.49
<b>80</b>	8.3	1.77	3.77

*Table 14 - The maximum preloading force of the gap and the maximum height of the closable gap*

From table 15 it is clear that a maximum gap of 10 mm cannot be closed only through the flexibility of the foundation pile and jacket leg by applying a preload. Therefore the gap has to be filled with a(n) (reinforced) epoxy resin.

## **6. Discussion and recommendations**

In 6.1 an interpretation of the results is given while in paragraph 6.2 recommendations for further development proposed.

### **6.1 Interpretation of the results**

First of all the result of the screw thread connection is a little bit less far developed than expected from the beginning of the thesis. To get a good solution for the jacket leg to foundation pile connection more research is done to different concepts as was foreseen. Other interpretations of the results are given below.

The screw thread connection can also be applied for a four-legged jacket. In a three-legged jacket the vertical difference in height between the foundation piles gives always a flat plane with an angle. In a four-legged jacket this is not always the case. Due to the rotation of the connector this problem is solved. The starting point was to find an option which could be applied for a three-legged jacket.

For the screw thread connection, the installation tolerance requirements from the installation company were reduced. This was determined at the end of the concept study. When this was also applied for the other concepts probably other concepts could have been more feasible as well. This does not mean that all the concepts have to be reconsidered. A lot of concepts were not rejected due to the large rotational tolerances.

The installation tolerances which are given from a contractor in the offshore wind industry are based upon the grouted connection. There is no need for more accurate installation tolerances for a grouted connection. So the foundation piles can be probably more accurately installed. Therefore the tolerances delivered from the contractor are more an indication of the maximum tolerances. The exact possible installation tolerances are not known, but a reduction is made.

The whole screw thread connection fulfills the ultimate limit state. From the unity checks of the hand calculations it is sure that the ultimate limit state will not be decisive because most of them are well below 1. The fatigue in the screw thread requires special attention, the damage of 5.6 has surely to be taken seriously. But it is possible that in this thesis the fatigue detail for the screw thread is taken a bit too conservative, so that in this situation a high damage indicates a point of attention. Also special attention needs to be given to the fatigue next to the holes of the foundation piles due to the nuds in the foundation piles because the unity check is also higher than 1.0.

## **6.2 Recommendations for further development**

To develop the screw thread connection some points for further developments are proposed. The first point is the fatigue in the screw thread. As a result from this thesis the screw thread in the connection is the section of the connection which is the most likely for a failure. However, the exact damage is very uncertain. It is important that both on the structural side as well on the load side more certainty is gained. On the structural side more certainty can be gained from tests and on the load side more certainty can be gained from a load spectrum for fatigue from a contractor applied to the screw thread connection. Also the influence of the tolerances of the screw thread on the fatigue in the screw thread connection has to be investigated.

Furthermore the filling with epoxy resin of the space between the foundation pile and the connector is a special point of attention. The viscosity of the epoxy resin is important as well as the sealing of the space between the connector and the foundation pile. Furthermore the storage for the epoxy resin, in- and outflow channels have to be designed.

Another point of investigation are the actuators. In case of a preloaded connection the actuators have to be investigated and the way that they are attached to the outer flange of the connector.

## **7. Conclusions**

The state of the art grouted connection uses a lot of unnecessary steel and grout and has a long installation time. The installation time can be reduced up to 75 percent by using a wedge connection. For a three-legged jacket substructure at least 18 m<sup>3</sup> of grout can be saved and the foundation piles do not have to be cleaned at the inside anymore.

The current installation tolerances are maximum 75 mm in the horizontal plane and maximum 50 mm in the vertical direction. The vertical results in the jacket rotation of 0.26 degrees. The maximum tilt of the foundation piles is 0.56 degrees.

With the tolerances supplied from the offshore industry 23 concepts were proposed to overcome the installation tolerances. These solutions can be roughly under divided in four groups. From which the screw thread connection is the best solution based on a multi-criteria analysis applied to the best concept of each of the four groups.

The screw thread connection does perform well for the ultimate limit state and the fatigue limit state. All the unity checks are equal or below 0.93 based on net stress, contact stress and bending stress for 10 different sections. The fatigue limit state needs more investigation, especially the fatigue in the screw thread which has a damage of 5.6. The other three sections have a damage around or below 1.0.

## 8. References

- Anderson, M. C. (2017). *The Hybrid Monopile*. Retrieved from <https://repository.tudelft.nl/islandora/object/uuid%3Ab67deab1-d5fd-46ea-9a8f-765d3cdf2485>
- CBS. (2017). Aandeel hernieuwbare energie 5,9 procent in 2016. Retrieved from <https://www.cbs.nl/nl-nl/nieuws/2017/22/aandeel-hernieuwbare-energie-5-9-procent-in-2016>
- Chen, I. W., Wong, B. L., Lin, Y. H., Chau, S. W., & Huang, H. H. (2016). *Design and Analysis of Jacket Substructures for Offshore Wind Turbines*. Retrieved from [https://www.researchgate.net/publication/299653209\\_Design\\_and\\_Analysis\\_of\\_Jacket\\_Substructures\\_for\\_Offshore\\_Wind\\_Turbines](https://www.researchgate.net/publication/299653209_Design_and_Analysis_of_Jacket_Substructures_for_Offshore_Wind_Turbines)

- Deep C Pile Group. (n.d.). Deep C Pile Dredging. Retrieved from <http://www.deepcgroup.com/dredging-trenching/deep-c-pile-dredging/>
- DFI. (2013). P-Y Curves : Models. Retrieved from <http://www.findapile.com/p-y-curves/p-y-curves-models>
- DNV GL. (2014). Design of Offshore Wind Turbine Structures - DNV-OS-J101. Retrieved from <https://rules.dnvgl.com/docs/pdf/DNV/codes/docs/2014-05/Os-J101.pdf>
- DNV GL. (2017a). RECOMMENDED PRACTICE DET NORSKE VERITAS DNV-RP-C205, Environmental conditions and environmental loads. Retrieved from <https://www.dnvgl.com/oilgas/download/dnvgl-rp-c205-environmental-conditions-and-environmental-loads.html>
- DNV GL. (2017b). Transport and installation of wind power plants - DNVGL-ST-0054. Retrieved from <http://rules.dnvgl.com/docs/pdf/DNVGL/ST/2017-06/DNVGL-ST-0054.pdf>
- Engineers Edge. (2000). External Metric ISO Thread Table Chart Sizes M260 - M1060. Retrieved from <https://www.engineersedge.com/hardware/metric-external-thread-sizes8.htm>
- Hoving, J.S. (2017a). L02 &03: - Intro Exercise, Substructure Design & Workshop: Bottom founded offshore structures. Lecture slides. TU Delft.
- Hoving, J.S. (2017b). L06 &07: Quasi-statics of towers and jackets: Bottom founded offshore structures. Lecture slides. TU Delft.
- Nijgh, M. P., Xin, H., & Veljkovic, M. (2018). Non-linear hybrid homogenization method for steel-reinforced resin. *Elsevier*, .
- Rijksoverheid. (n.d.). Windenergie op zee. Retrieved from <https://www.rijksoverheid.nl/onderwerpen/duurzame-energie/windenergie-op-zee>
- Rijksoverheid. (2018). Windenergie op zee. Retrieved from <https://www.rijksoverheid.nl/onderwerpen/duurzame-energie/windenergie-op-zee>
- Seidel, M. (2018). Tolerance requirements for flange connections in wind turbine support structures. *Stahlbau*, . Retrieved from [https://www.researchgate.net/publication/327439584\\_Tolerance\\_requirements\\_for\\_flange\\_connections\\_in\\_wind\\_turbine\\_support\\_structures](https://www.researchgate.net/publication/327439584_Tolerance_requirements_for_flange_connections_in_wind_turbine_support_structures)
- Van Oord. (2017). Van Oord signs contract for East Anglia ONE offshore windfarm. Retrieved from <https://www.vanoord.com/news/2017-van-oord-signs-contract-east-anglia-one-offshore-windfarm>
- Vugts, J. H. (2016). *Handbook of Bottom Founded Offshore Structures - Part 1. General features of offshore structures and theoretical background* (Rev. ed.). Delft, The Netherlands: Eburon.
- ZUNO Stroom Atlas. (n.d.). Wetwetwet - Zuno current map. Retrieved from <http://www.wetwetwet.nl/zunostroomatlas/index.php?lang=nl>

## **Appendix A: Graph to use for the displacement of the foundation pile**

Graphs to determine soil parameters in the p-y curves (DNVGL, 2014).

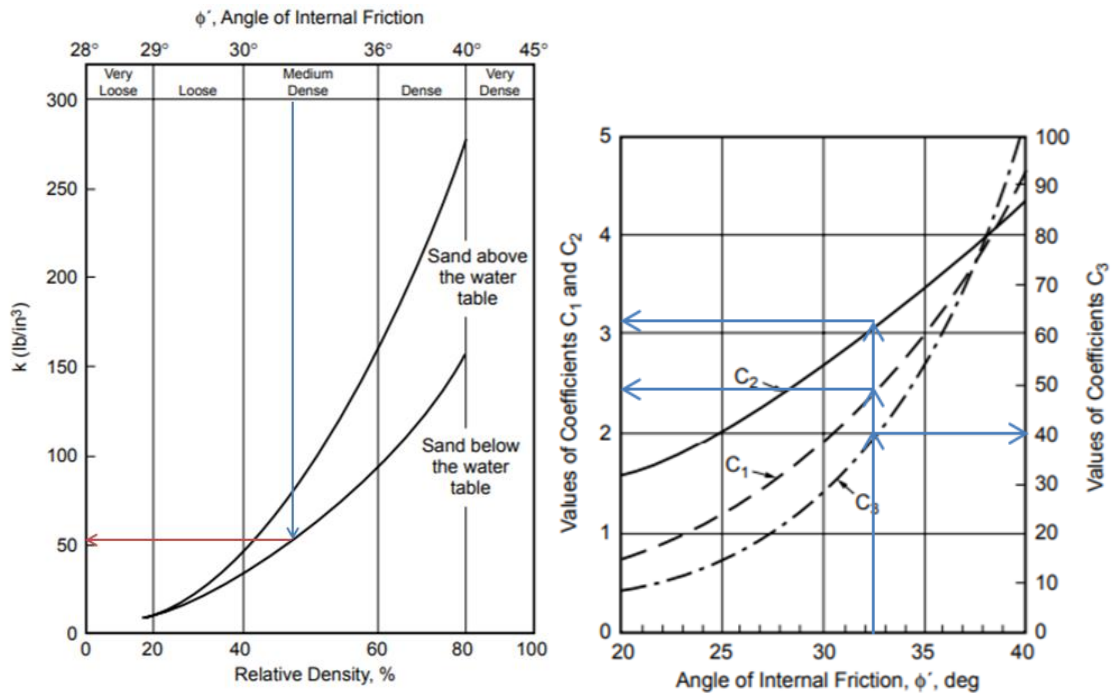


Figure 53 - Graphs to determine the soil parameters

## Appendix B: Installation loads on the screw thread connection

In this appendix the installation loads on the screw thread connection are determined to investigate the maximum required torquing moment and the load to bend the foundation piles. First of all a reference project is chosen. Secondly the dimensions of the jacket structure

are determined. After that the horizontal and vertical forces acting at the jacket structure are defined. To calculate the vertical load, the weight of the jacket is determined and the volume of the jacket structure below sea-level. To calculate the horizontal load, the Morison's equation is applied. To know all the variables in the Morison's equation, the current, velocity and acceleration profile over the height of the jacket structure are determined. Subsequently an equivalent diameter of the jacket is determined by a stick model. The coefficients for drag and inertia are now determined and finally the horizontal load is calculated according to Morison's equation. The last step is to calculate the support reactions.

### Reference project

East Anglia one is chosen as a reference project. East Anglia one is a wind farm forty kilometers from the east coast of England which is still under construction and will be completed in 2020. The wind farm will exist of 102 wind turbines with for all the wind turbines a capacity of 7 MW. The wind farm will provide electricity to almost 600,000 homes. All of the wind turbines are installed on three-legged jacket structures, which have a height of 65 meters. The average water depth is 45 meters (Van Oord, 2017). To determine the installation loads at the wedge connection, a wind turbine of 10 MW and a water depth of 60 meters are used as a reference to make the calculation also applicable to possible larger jacket structures in the future.

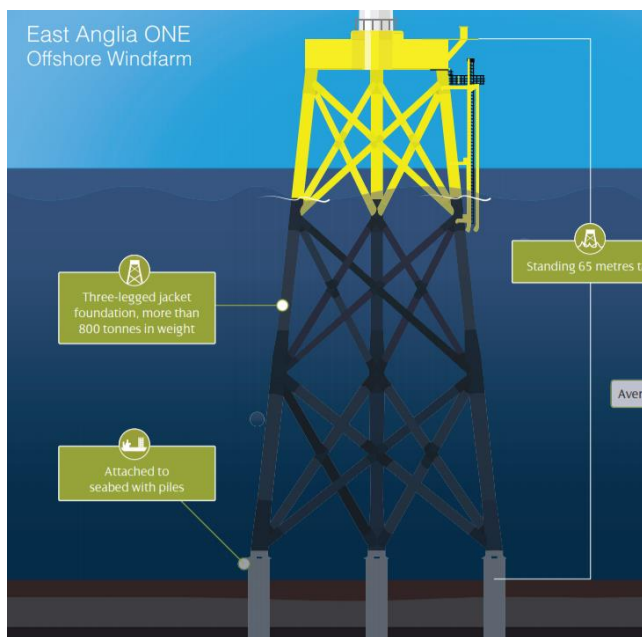
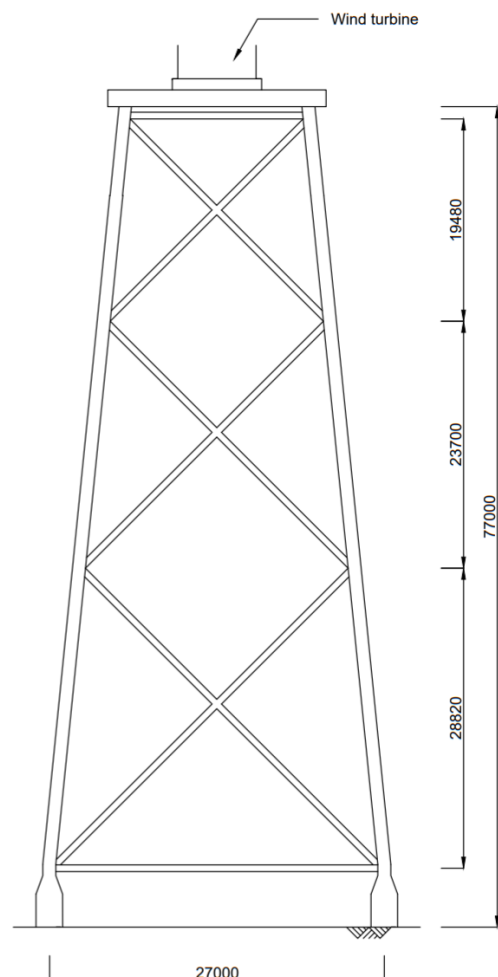


Figure 54 - Jacket structure of East Anglia one

### Geometry of the jacket structure

The jacket structure is a three-legged jacket structure, to make all the wedge connection concepts



suitable for implementation into the jacket to foundation pile connection. With a water depth of 60 meters, the minimum height of the jacket structure is given as:

$$H_{jacket} = \text{Mean sea level} + \text{Higher Astronomical Tide (HAT)} + 0.5 * \text{wave height} + \text{Surge} + \text{Airgap} \rightarrow H_{jacket} = 60 + 1.0 + 8.0 + 2.25 + 1.5 = 72.75 \text{ m}$$

Including the stick-up length of the foundation pile and the connection the total height of the jacket will be approximately 77 meters. The horizontal top braces are 8 meters above sea level to prevent fatigue in the brace by wave loading (J.S. Hoving, 2017a). The brace patterns will consist of x-bracings. This is a common pattern for offshore wind jacket structures. Further is the width of the bottom brace is given to be 27 meters while the width of the upper horizontal brace is assumed to be 15 meters. These are the only horizontal braces. From the lengths of the horizontal braces follows that the batter angle of the jacket structure is 1:8.66.

The diameter of the jacket legs is assumed to be 1.5 meter. The ratio of the diameter divided by the wall thickness of the jacket leg is generally taken as  $D/t = 30$ . This gives  $t = 0.050$  m, which is around 3 cm. The geometry of the bays in the jacket structure has the same ratio. The assumed height for the bays is 72 meters. To get the angle of the x-bracings around 45 degrees with the horizontal, the jacket structure will exist of three bays. The scale factor of the geometry of the bays is determined by the following formula. The scale factor is:

Figure 55 - Dimensions for of the reference offshore jacket

$$m_{jacket} = \left( \frac{b_{N_b}}{b_0} \right)^{1/N_b} \rightarrow m_{jacket} = \left( \frac{27}{15} \right)^{1/3} = 1.216$$

As said, all the bays are given the same relative geometrical dimensions and are only enlarged by  $m_{jacket}^{N_b}$ . Therefore yields:

$$h_{tot,bays} = h_1 + m_{jacket} * h_1 + m_{jacket}^2 * h_1 \rightarrow h_1 = 19.48, h_2 = m_{jacket} * h_1 = 23.70 \text{ and } h_3 = m_{jacket}^2 * h_1 = 28.82$$

In which  $h_1$  is the height of the upper bay,  $h_2$  is the height of the middle bay and  $h_3$  is the height of the lower bay.

The proportions between the height and length of a bay are given as  $\frac{h_{N_b}}{h_{N_b-1}} = \frac{b_{N_b}}{b_{N-1}}$ .

From this follows that  $b_1 = 18.24$  and  $b_2 = 22.18$ . With the values for  $b_1$  and  $b_2$  the angle with the horizontal for the diagonal braces can be defined. This angle is:

$$\theta_{odd} = \frac{h_{N_b-1}}{b_{N_b} - (b_{N_b} - b_{N_b-1})/2} = 49.5 \text{ degrees.}$$

All the diagonal braces have an angle of 49.5 degrees with the horizontal.

To determine the diameter of the braces the rule of thumb is applied. A first approximation for the diameter of the diagonal braces is given by:

$$D_{br,d} = 0.018 * L_{br,d}$$

The average length of a diagonal brace is  $\sqrt{28.82^2 + 24.59^2} = 37.9 \text{ m}$ . By using the rule of thumb this results in a diameter of 0.7 meter. The ratio of the diameter divided by the wall thickness of the x-bracings is taken as  $D/t = 30$  (J.S. Hoving, 2017a). So the wall thickness of the diagonal braces is 0.02 meter. This is taken to be 2.5 centimeters to be conservative.

The following rule of thumb is applied to find a diameter for the horizontal braces:

$$D_{br,h} = 0.023 * L_{br,h}$$

The length for a horizontal brace is maximum 27 meter. This implies that the diameter is 0.70 meter. Here yields the same as rule of thumb for the wall thickness of the horizontal braces. And therefore the wall thickness for the diagonal braces is also 2.5 centimeter. Now the whole geometry of the jacket structure is determined and the loads working from and on the jacket structure can be determined.

### Loads acting at the offshore jacket structure

The loads which are applied to the jacket structure can be divided in the following categories:

Vertical forces:

- The self-weight of the jacket
- The buoyancy force of the water

Horizontal forces:

- The wave load on the jacket
- The current load on the jacket
- Wind load on the top side of the jacket structure (This load is neglected, because the installation of the jacket structure is not allowed by strong winds)

The forces from all these categories are elaborated in the next pages.

### Vertical forces

#### The self-weight of the jacket structure

The self-weight of the jacket structure can be determined because the geometry of the jacket structure is known. The length of the members of the jacket structure are summarized in table 16.

	$L_{bay,1}$ (m)	$L_{bay,1}$ (m)	$L_{bay,2}$ (m)	$L_{bay,3}$ (m)	Diameter (m)	Thickness (m)
<b>Leg</b>	-	19.61	23.86	29.02	1.50	0.050
<b>Horizontal bracing</b>	15	0	22.20	27	0.70	0.025
<b>Diagonal</b>	-	25.60	31.14	37.89	0.70	0.025

<b>bracing</b>						
----------------	--	--	--	--	--	--

Table 15- Dimensions of the jacket

In addition to already known the jacket geometry a top surface with a thickness of 20 centimeter on top of the three jacket legs is assumed to carry the wind turbine. The area of the top surface is  $15 \times 15 / 2 = 62.5 \text{ m}^2$ . This gives a volume for the top surface of  $0.20 \times 62.5 = 12.5 \text{ m}^3$ . The weight of the top surface of the jacket structure is  $7850 \times 12.5 = 98125 \text{ kg} = 1.0 \text{ MN}$ .

The bottom part of the wind turbine is also attached already to the jacket structure. This is called the turbine foot. This turbine foot has a diameter of 8.3 meter and a wall thickness 100 mm and a height of 2.5 meter. These geometrical properties are given from a 10 MW turbine. The volume of the turbine foot is  $\pi * D_{conn,tower} * t_{conn,tower} * t_{conn,tower} = \pi * 8.3 * 0.10 * 2.5 = 6.5 \text{ m}^3$ . The weight of the turbine foot is equal to:  $6.5 * 7850 = 51172 \text{ kg} = 0.51 \text{ MN}$ . So the total jacket top weight is 1.49 MN.

In table 17 the length of the members of the jacket structure are added together. From the total length of the different members the total weight of members is determined. By adding the weight of the top surface and of the turbine foot of the wind turbine to the weight of the members, the total weight is found to be 8.5 MN.

	<b>Total length(m)</b>	<b>Weight (MN)</b>
<b>Leg</b>	217.5	4.0
<b>Horizontal bracing</b>	126	0.54
<b>Diagonal bracing</b>	567.8	2.45
<b>Top surface</b>	-	1.0
<b>Foot of turbine</b>	-	0.51
<b>Total</b>	-	8.5

Table 16 - Weight of several components of the jacket structure

### Buoyancy on the jacket

The buoyancy force on the jacket is given by the volume of the jacket structure under water level. The jacket is assumed to be filled with air because the tubulars are welded together onshore. However a reduction factor of 0.8 is applied for potential leakages. The volume of the jacket below water level is given by:

$$\begin{aligned}
 V_{jacket, bel, wat} &= \left( \frac{\pi}{4} * D_{br,d}^2 * L_{br,d} + \frac{\pi}{4} * D_{br,h}^2 * L_{br,h} + \frac{\pi}{4} * D_{leg}^2 * L_{leg} \right) \rightarrow V_{jacket, bel, wat} \\
 &= \left( \frac{\pi}{4} * 0.70^2 * 6 * \left( 37.9 + 31.14 + 25.6 * \frac{2980}{19480} \right) + \frac{\pi}{4} * 0.70^2 * 3 * 27 + \frac{\pi}{4} \right. \\
 &\quad \left. * 1.5^2 * 3 * \left( \frac{60.3}{60} * 57 \right) \right) = 503.3 \text{ m}^3
 \end{aligned}$$

So the buoyancy force of the whole jacket is given by:

$$\begin{aligned}
 F_{buoyancy} &= r_{buoy} * \rho_{water} * V_{jacket, bel, water} \rightarrow F_{buoyancy} = 0.8 * 1000 * 503.3 \\
 &= 4.0 \text{ MN upwards}
 \end{aligned}$$

The combination of self-weight of the jacket and buoyancy gives a force of 4.5 MN downwards. This is 1.5 MN per jacket leg.

### **Horizontal forces**

The horizontal loads applied at the jacket structure are a combination from the current and the waves at location of the structure. The waves and the current result in a horizontal movement of the water particles. Therefore they can be added together in the calculation of the horizontal load applied to the jacket structure. The horizontal force is split in two components: A drag component for the resistance to the flow and an inertia component for the resistance to the local acceleration of the water particles. In the end the final horizontal force can be calculated with the known Morison equation.

$$F_{Morison} = F_I + F_d = C_m * \frac{1}{4} * \rho_{water} * D^2 * \dot{v} + C_d * \frac{1}{2} * \rho_{water} * D * v * |v|$$

With:

$C_m =$  Mass coefficient

$C_D =$  Drag coefficient (constant)

Morison's equation may only be applied if  $\lambda > 5D_{leg}$ . The wave lengths should be larger than 7.5 meter. This is the case, so Morison's equation can be applied. The longitudinal dimensions of the members in the jacket are much larger than their transverse dimensions. Therefore the end effects may be ignored. (DNV GL, 2017a)

To find the horizontal load on the jacket structure, a vertical profile of the horizontal water velocity, water acceleration and equivalent diameter of the jacket structure have to be determined. Also the constants for drag and inertia have to be defined for the different members of the jacket.

### Stick model

To calculate the wave and current load on the jacket structure, the jacket structure is simplified by the stick model. The idea of the stick model is to represent all the diameters of all the different members as an equivalent diameter in one model. The model replaces the real structure and all the loads are acting on the model with the equivalent diameter. The equivalent diameter can vary over the height of the jacket structure, dependent on the braces in the jacket structure. All the members off the jacket structure have a contribution in the equivalent diameter of the stick model. The equivalent diameter for the calculation of the inertia force is different from the equivalent diameter to calculate the drag force. The jacket structure is therefore represented by two stick models. One model to calculate the drag force and another model to calculate the inertia force.

To calculate the maximum force on the jacket structure, the waves and the current are assumed to have the same direction. To calculate the horizontal load, two situations are assumed. Both situations give another load on the jacket structure. Both situations can happen, but will never occur simultaneously. In figure 68 the top view of the load on the jacket structure is given for the two situations.

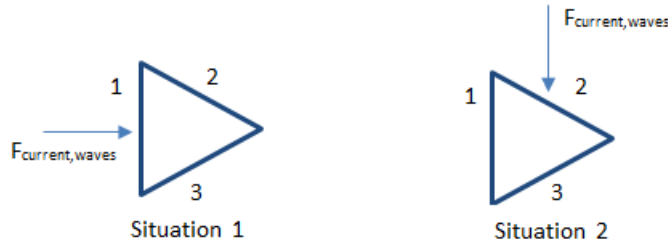


Figure 56 - Top view of the jackets with the current and the wave direction in two situations

In both cases the braces are differently orientated to the waves and current and will therefore give a different equivalent diameter in the stick model (Vugts, 2016). In both situations the sides 2 and 3 will give the same contribution to the equivalent diameter for drag as well as for inertia load.

To simplify the model the assumption is made that the jacket legs have a perfect vertical orientation. Also the braces can have only an inclination in a horizontal or a vertical plane (so the batter angle is ignored). In the table 18 the contribution of all the members to the equivalent diameter for drag and inertia load for situation 1 are given.

	Drag		Inertia	
	$D_{eq,side1}$	$D_{eq,side2,3}$	$D_{eq,side1}$	$D_{eq,side2,3}$
<b>Hor. brace</b>	$L_{br,h}$	$L_{br,h} * \sin(\mu_{jacket})^3$	$\sqrt{D_{br,h} * L_{br,h}}$	$\frac{\sin(\mu_{jacket})}{* \sqrt{D_{br,h} * L_{br,h}}}$
<b>Diag. brace</b>	$\frac{D_{br,d}}{\sin(\theta_{odd})}$	$1.14 * D_{br,d}$	$D_{br,d} / \sqrt{\sin(\theta_{odd})}$	$1.07 * D_{br,d}$
<b>Jacket leg</b>	$D_{leg}$	$D_{leg}$	$D_{leg}$	$D_{leg}$

Table 17 - Equivalent diameters for the members of the jacket in situation 1

Substituting values into table 18 delivers the following diameters:

	Drag		Inertia	
	$D_{eq,side1} (m)$	$D_{eq,side2,3} (m)$	$D_{eq,side1} (m)$	$D_{eq,side2,3} (m)$
<b>Hor. brace</b>	27	3.38	4.35	2.17
<b>Diag. brace</b>	0.92	0.80	0.80	0.75
<b>Jacket leg</b>	1.5	1.5	1.5	1.5

Table 18 - Equivalent diameters for the jacket in situation 1 in numbers

Since the contribution of all the jacket members to the equivalent diameters is known, the equivalent diameters can to be plotted. The equivalent diameter to calculate the drag force is plotted in figure 69 (left) and the equivalent diameter to calculate the inertia force is plotted in figure 69 (right).

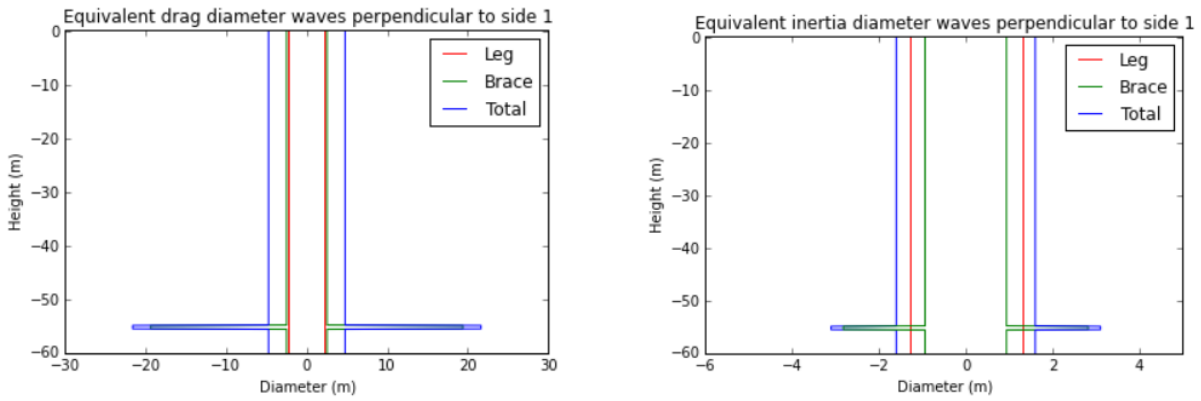


Figure 57 - Equivalent drag diameter (left) and equivalent inertia diameter (right)

By doing the same procedure for situation 2 the following tables and plots are obtained.

	Drag		Inertia	
	$D_{eq,side1}$	$D_{eq,side2,3}$	$D_{eq,side1}$	$D_{eq,side2,3}$
<b>Hor. brace</b>	0	$L * \sin(\mu_{jacket})^3$	0	$\sin(\mu_{jacket}) * \sqrt{D_{br,d}}$
<b>Diag. brace</b>	$D_{br,d}$	$1.1 * D_{br,d}$	$D_{br,d}$	$1.05 * D_{br,d}$
<b>Jacket leg</b>	$D_{leg}$	$D_{leg}$	$D_{leg}$	$D_{leg}$

Table 19 - Equivalent diameters for the members in situation 2

	Drag		Inertia	
	$D_{eq,side1}$	$D_{eq,side2,3}$	$D_{eq,side1}$	$D_{eq,side2,3}$
<b>Hor. brace</b>	0	17.54	0	0.72
<b>Diag. brace</b>	0.7	0.77	0.7	0.74
<b>Jacket leg</b>	1.5	1.5	1.5	1.5

Table 20 - The equivalent diameters for situation 2 in numbers

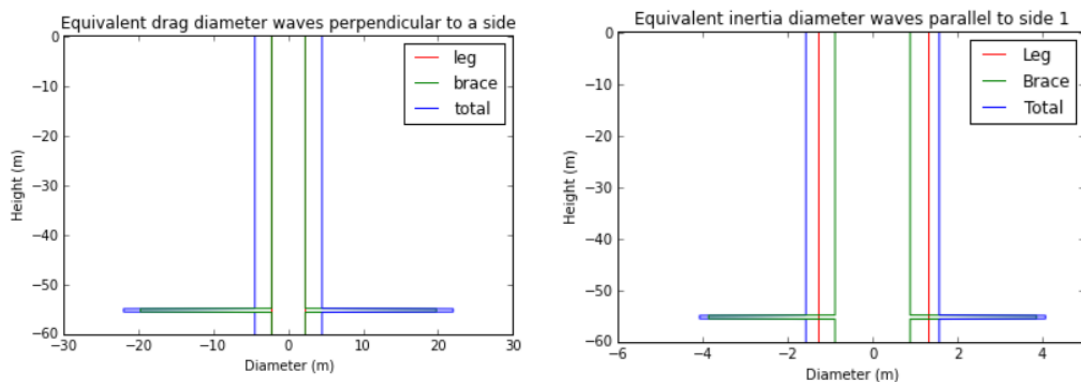


Figure 58 - Equivalent drag diameter (left) and equivalent inertia diameter (right)

The vertical velocity profile of the horizontal wave velocity

Surface waves at sea can be divided in three categories: Waves in deep water, waves in intermediate water depths and waves in shallow water. In deep water the wavelength and the motion of the water particles are not influenced by the bottom. This results in an orbital motion of the water particles (figure 71). The horizontal and vertical

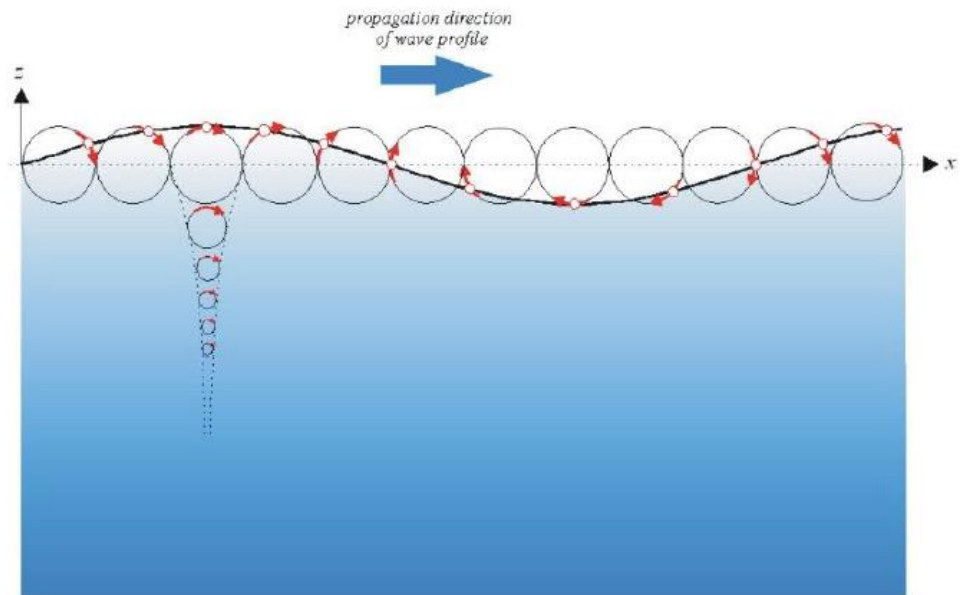


Figure 59 - Circular motion of water molecules over depth

velocity due to the waves is zero at the bottom. At intermediate water depths the motion of the water particles are influenced by the bottom. The movement of the water particles becomes more elliptical and the decay of the horizontal velocity of the particles along the depth is less than in deep water. The shallower the water and the closer to the sea bed, the more the motion of a water particles is elliptical. At the seabed only a horizontal motion of water particles occurs. In shallow water the wavelength is only dependent on the depth of the water and the movement of the water particles is elliptical along the whole water depth.

The allowable wave height during the installation is assumed to be 1 meter. The corresponding period of this wave is 4.3 seconds (Anderson, 2017). The corresponding wavelength is given by:

$$\lambda = \frac{gT^2}{2\pi} * \tanh\left(\frac{2\pi d}{\lambda}\right)$$

The wave length is 28.84 m. The wavelength should not exceed two times the water depth to be classified as deep water. In this case yields: 28.82 meter < 120 meter. Therefore a wave with a height of 1 meter at a water depth of 60 meters in the North Sea is categorized as a wave in deep water. Now the maximum horizontal velocity depth decay function for deep water is given by:

$$Decay(z) = \omega * a * \frac{\cosh k(z + d)}{\cosh(kd)}, -d \leq z \leq 0 \quad (\text{for Airy waves})$$

The maximum horizontal acceleration profile is given by:

$$accelaration(z) = \omega^2 * a * \frac{\cosh k(z + d)}{\cosh(kd)}, -d \leq z \leq 0$$

Where:

$k = \text{wavenumber } (2\pi / \lambda)$

These results of the vertical profile of the horizontal velocity and acceleration are depicted in figure 72.

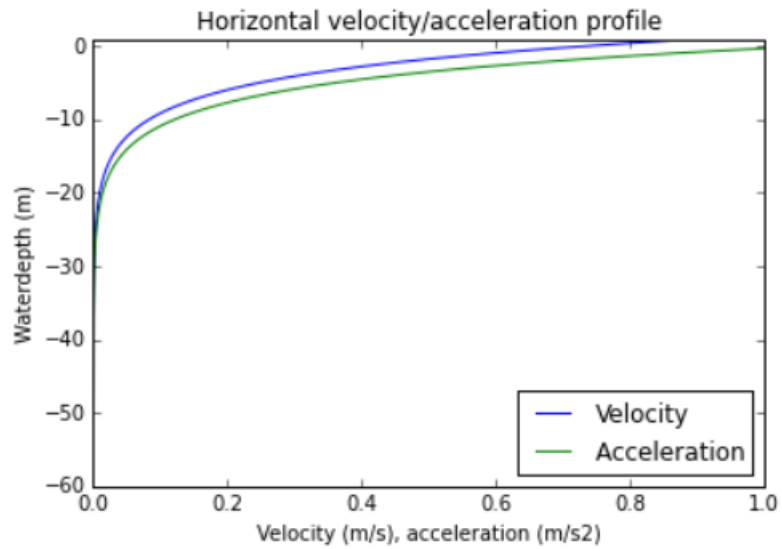


Figure 60 - Horizontal velocity profile over water depth

The maximum horizontal velocity and acceleration are assumed to be working at the same time at all the members of the jacket. This is a conservative, but an easy assumption.

#### The current at the location of the jacket

The current at the surface the North Sea is obtained (ZUNO Stroom Atlas, z.d.). From figure 73 it is clear that the current at the location of the jacket structure (red star) is about 2.3 knots (figure 73). This is equal to 1.0 m/s.

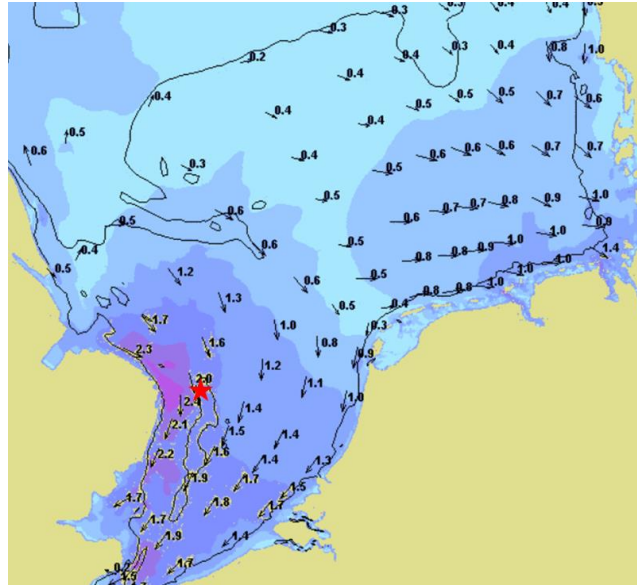


Figure 61 - Maximum current at water surface of the North Sea during average tide in knots

The current has a maximum horizontal velocity at the water surface and a minimum velocity at the seabed. At the seabed the horizontal velocity is zero. The horizontal velocity profile for the current is given by the following formula:

$$v_{c,tide}(z) = v_{c,tide}(0) * \left(\frac{d+z}{d}\right)^{\alpha_{c,tide}} \text{ for } z \leq 0$$

With:

$v_{c,tide}(0)$  = the tidal current velocity at the sea surface

$\alpha_{c,tide}$  = exponent – typically  $\alpha_{c,tide} = 1/7$

By plotting this formula over the water depth at the location of the jacket structure, figure 74 is obtained.

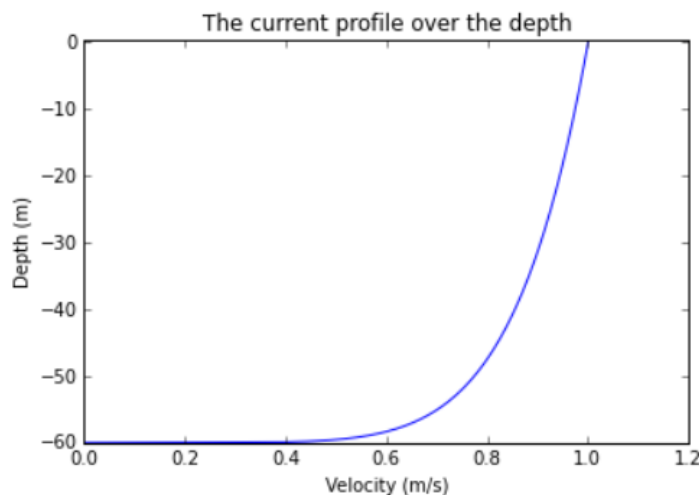


Figure 62 - The horizontal velocity of the current profile at the location of the jacket

The horizontal velocity from the current from the waves

The horizontal velocity profile from the waves and the current can be added. The maximum horizontal velocity occurs at the sea surface and the minimum velocity at the seabed. From figure 75 can be seen that the average horizontal velocity is around 1 meter per second. For an indicative calculation for the Reynolds number, the value for the horizontal velocity of 1 meter per second of the water is a good enough approximation.

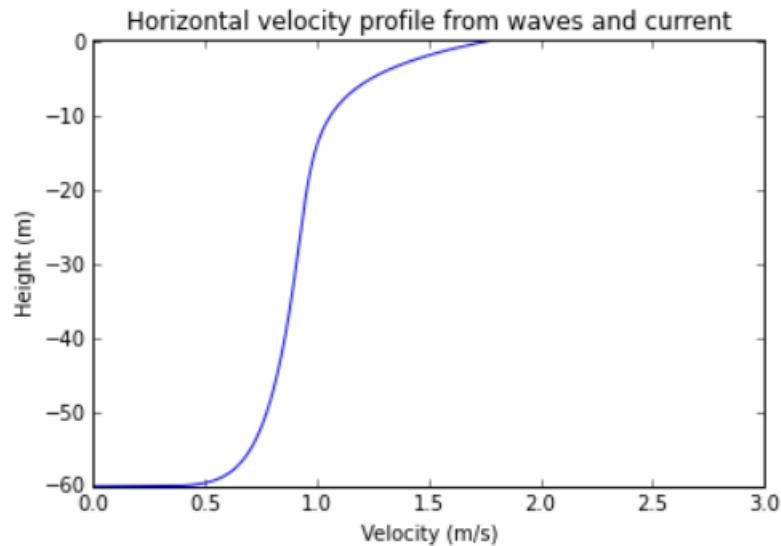


Figure 63 - Total horizontal water profile at the location during installation

Since the equivalent diameter, velocity and acceleration profile are known already, only the  $C_m$  and  $C_D$  - coefficients have still to be determined.

$C_m$ - coefficients

According to the DNV rules the coefficient for inertia is given by the following formulas:

$C_m = 1 + C_a$ , with  $C_a = \frac{m_a}{\rho_{water} * A_{full}}$ , which gives different values for  $C_m$  for the different diameters of the different jacket members. The  $C_m$  - coefficient for the jacket legs is 1.98, while the  $C_m$  - coefficient of the braces is 3.03.

$C_D$ - coefficients

At the moment of installation the surfaces of the jacket structure are coated. The surface roughness for several materials is given in figure 76.

Table 6-1 Surface roughness	
Material	$k$ (meters)
Steel, new uncoated	$5 \times 10^{-5}$
Steel, painted	$5 \times 10^{-6}$
Steel, highly corroded	$3 \times 10^{-3}$
Concrete	$3 \times 10^{-3}$
Marine growth	$5 \times 10^{-3} - 5 \times 10^{-2}$

Figure 64 - Different  $k$ -values for different materials (DNV GL, 2017a)

From figure 76 follows that the value of the roughness  $k$  is  $5 * 10^{-6} m$ . Since the diameter of the jacket members in the structure is taken to be 1 meter in this calculation, the value of  $\Delta = k/D$  is also  $5 * 10^{-6}$ . To determine the  $C_d$ - coefficients for the jacket legs and braces, the Reynolds number has to be calculated first.

### Reynolds number

The Reynolds number is an important number to predict flow patterns. A Reynolds number below 4000 indicates a laminar flow. And a Reynolds number larger than 4000 indicates a turbulent flow. The Reynolds number is calculated by the following formula:

$$Re = \frac{v * L * \rho_{water}}{\mu_{water}} = \frac{v * L}{\nu_{water}} \rightarrow \frac{1 * 1}{1.3 * 10^{-3}} = 7.7 * 10^5$$

The dynamic viscosity of the water at a temperature of 10 °C is:  $\mu_{water} = 1.3 * 10^{-6} m/s^2$

$L$  = Diameter of the members (average 1 m)

$v$  = horizontal velocity of the water (1 m/s near the surface level of the sea)

From this large Reynolds number it is clear that the water flow is turbulent along the height of the jacket structure.

In figure 77 the  $C_d$ - coefficients are given for several values for  $\Delta$ . From this figure and the Reynolds number follows that the  $C_d$ - coefficients for both the jacket legs and the braces is approximately 0.3.

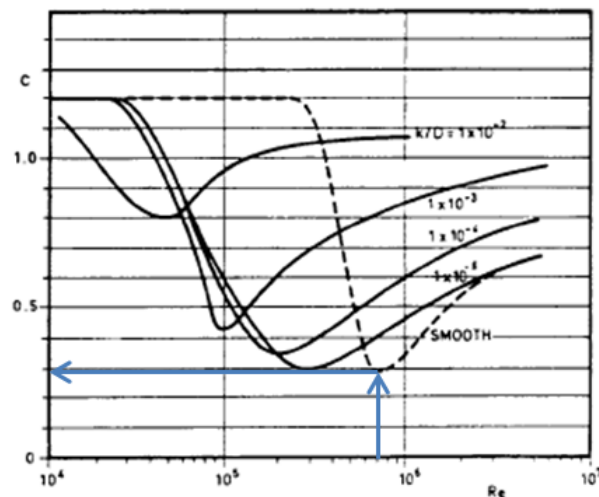


Figure 65 - Graph to determine the  $C_d$ -coefficient

### Calculation of the total horizontal force

All the information which is necessary to calculate the horizontal force over the vertical height of the jacket structure is determined. Now the Morison's equation can be applied over the full height of the jacket structure. This results for situation 1 and situation 2 in different forces and different moments at the base of the jacket. In figure 78 the force per meter height of the jacket structure is shown for the situations 1 and 2 respectively.

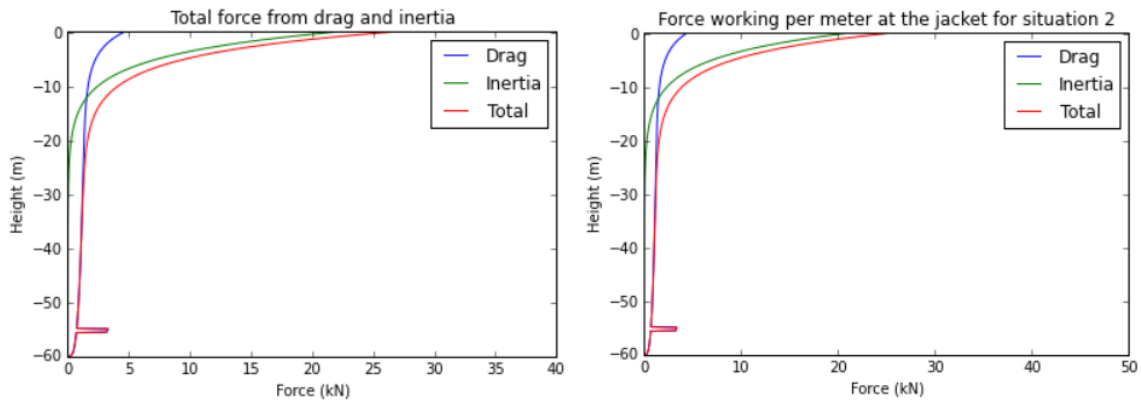


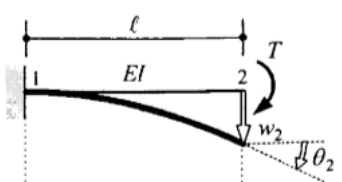
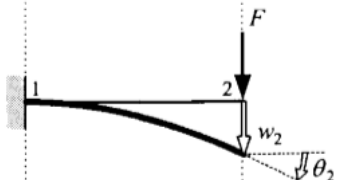
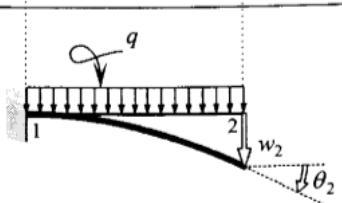
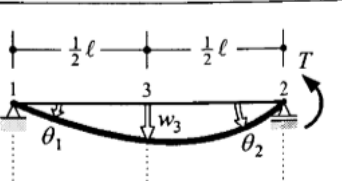
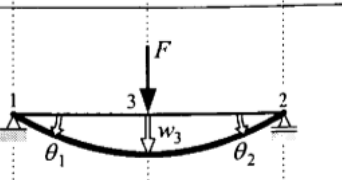
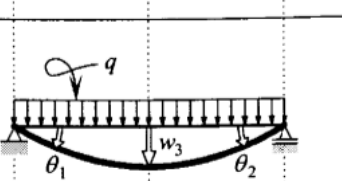
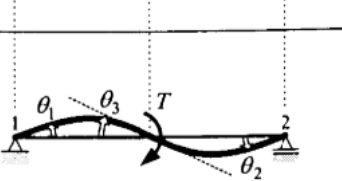
Figure 66 - Horizontal loads on jacket situation 1 (left) and for situation 2 (right)

The total horizontal load applied to the jacket structure can be determined by taking the integral of all the forces over the height of the jacket. By multiplying the total horizontal force with the total distance and dividing it by the resultant of the horizontal force, the location of the resultant force is determined. The overturning bending moment is calculated by multiplying the distance from the resultant force to the connection by resultant of the horizontal force. The vertical support reactions are determined by dividing the bending moment over the distance from the rotation center to the foundation piles. All these results are summarized in table 22. From this table the maximum load is given by the situation 1.

	<b>Situation 1</b>	<b>Situation 2</b>
<b>Drag force</b>	82.7 kN	78.2 kN
<b>Inertia force</b>	106.1 kN	101 kN
<b>Total force</b>	188.8 kN	179.2 kN
<b>Bending moment</b>	8.55 MNm	8.12 MNm
<b>Force on the connection</b>	365.6 kN	300.7 kN
<b>Maximum reaction support</b>	1.87 MN	1.80 MN

Table 21 - Forces and maximum bending resistance

## Appendix C: Bending beam equations

(1)		$\theta_2 = \frac{Tl}{EI}; \quad w_2 = \frac{Tl^2}{2EI}$
(2)		$\theta_2 = \frac{Fl^2}{2EI}; \quad w_2 = \frac{Fl^3}{3EI}$
(3)		$\theta_2 = \frac{ql^3}{6EI}; \quad w_2 = \frac{ql^4}{8EI}$
(4)		$\theta_1 = \frac{1}{6} \frac{Tl}{EI}; \quad \theta_2 = \frac{1}{3} \frac{Tl}{EI}; \quad w_3 = \frac{1}{16} \frac{Tl^2}{EI}$
(5)		$\theta_1 = \theta_2 = \frac{1}{16} \frac{Fl^2}{EI}; \quad w_3 = \frac{1}{48} \frac{Fl^3}{EI}$
(6)		$\theta_1 = \theta_2 = \frac{1}{24} \frac{ql^3}{EI}; \quad w_3 = \frac{5}{384} \frac{ql^4}{EI}$
(a)		$\theta_1 = \theta_2 = \frac{1}{24} \frac{Tl}{EI}; \quad \theta_3 = \frac{1}{12} \frac{Tl}{EI}; \quad w_3 = 0$

vergeet-mij-nietjes

vrij opgelegde ligger (statisch bepaald)

Figure 67 - Bending beam equations

statisch onbepaalde ligger (enkelzijdig ingeklemd)	(7)		$\theta_2 = \frac{1}{4} \frac{T \ell}{EI}; \quad w_3 = \frac{1}{32} \frac{T \ell^2}{EI}$ $M_1 = \frac{1}{2} T; \quad V_1 = V_2 = \frac{3}{2} \frac{T}{\ell}$
	(8)		$\theta_2 = \frac{1}{32} \frac{F \ell^2}{EI}; \quad w_3 = \frac{7}{768} \frac{F \ell^3}{EI}$ $M_1 = \frac{3}{16} F \ell; \quad V_1 = \frac{11}{16} F; \quad V_2 = \frac{5}{16} F$
	(9)		$\theta_2 = \frac{1}{48} \frac{q \ell^3}{EI}; \quad w_3 = \frac{1}{192} \frac{q \ell^4}{EI}$ $M_1 = \frac{1}{8} q \ell^2; \quad V_1 = \frac{5}{8} q \ell; \quad V_2 = \frac{3}{8} q \ell$
statisch onbepaalde ligger (tweezijdig ingeklemd)	(10)		$w_3 = \frac{1}{192} \frac{F \ell^3}{EI}$ $M_1 = M_2 = \frac{1}{8} F \ell; \quad V_1 = V_2 = \frac{1}{2} F$
	(11)		$w_3 = \frac{1}{384} \frac{q \ell^4}{EI}$ $M_1 = M_2 = \frac{1}{12} q \ell^2; \quad V_1 = V_2 = \frac{1}{2} q \ell$
	(b)		$\theta_3 = \frac{1}{16} \frac{T \ell}{EI}; \quad w_3 = 0$ $M_1 = M_2 = \frac{1}{4} T; \quad V_1 = V_2 = \frac{3}{2} \frac{T}{\ell}$

Figure 68 - Bending beam equations

## Appendix D: Utilize elasticity between the jacket leg and foundation pile

An investigated option is to make a flexible connection between the connector and the jacket leg and to use its flexibility to bend the connector upon the foundation pile. The situation is shown in figure 81. The jacket leg is with a blade (leaf spring) connected to the connector. The blade is welded to the jacket leg and to the connector and may be assumed to be fixed at both ends. When the foundation pile and the jacket leg have a maximum rotational difference, the maximum difference in height of the top of the pile is 40 mm (figure 82). During the installation of the jacket, the connector is assumed to be horizontal. The connector will first touch the highest part of the foundation pile. By moving the jacket structure further

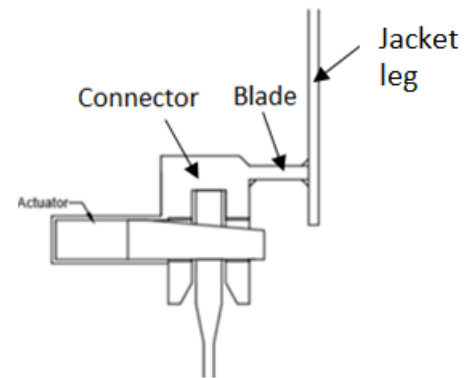


Figure 69 - Connection with deformation from elasticity

downwards the blade will start to deform. After maximum 40 mm deformation the whole connector touches the foundation pile as shown in figure 82 and the wedges can be installed.

The force which is needed to push the blade 40 mm downwards per meter length of spring is modeled by the bending beam equation in figure 83. In the bending beam equation  $w_0 = 40 \text{ mm}$ . The length of the blade  $l_{blade}$  is determined by the inner diameter of the connector minus the diameter of the jacket leg. The inner diameter of the connector is approximately 2.3 meter while the diameter of the jacket leg may vary between the 1.0 and 2.0 meter. This indicates that the length of the spring is between:

$$\frac{2.3-2.0}{2} = 0.15 < l_{blade} < \frac{2.3-1.0}{2} = 0.65$$

To check if this concept is a feasible, the required thickness is calculated for three requirements. If a thickness exists which fulfill all the requirements the concept is technical feasible. The blade has to fulfill the following three requirements:

1. The length of the blade is between the 0.15 and 0.65 meter based on the diameter of the jacket leg and the diameter of the foundation pile. No requirements for the thickness of the blade are imposed from the geometry.
2. The force which is applied during installation to the jacket leg should be able to give a vertical impression of the spring of 40 mm. The installation force which is applied to the connection is the self-weight minus the buoyancy force of the jacket. The self-weight of the jacket is 850 tons (Appendix B) while the buoyancy is 4.0 MN. So the installation force per jacket leg is maximum

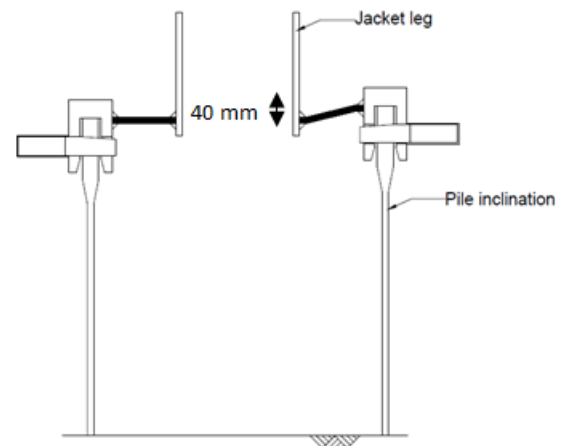


Figure 70 - 40 mm between pile edge left and right

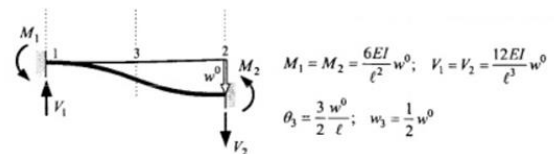


Figure 71 - The bending beam equation for the displacement in the leaf spring

1.50 MN. The length as a function of the thickness is given by the following equation derived from the bending beam equation in figure 83.

$$F_{net,selfw} = \frac{12EI_{zz,blade}}{l_{min,blade}^3} * W_0 \rightarrow l_{min,blade} = \sqrt[3]{\frac{12 * E * \frac{1}{12} * b * h_{blade}^3}{F_{net,selfw}} * W_0}$$

This is a lower bound solution for the length of the spring. When the blade is shorter than the length calculated above, the installation force is not sufficient to deform the blade 40 mm in vertical direction.

3. In maximum compression the stress in the blade have to stay below the yield stress which is assumed to be 460 MPa. The maximum length of the spring is also derived from the bending beam equation in figure 83 and is shown in the equation below for this criterion. Combining the two formulas for  $M_{max}$  gives:

$$M_{max,blade} = \frac{F_{Ed,comp} * l_{max,blade}}{2} \text{ and } M_{max,blade} = \frac{I_{blade} * f_y}{h_{blade}/2} \text{ gives } l_{max,blade} = \frac{2 * f_y * b * h_{blade}^2}{6 * F_{Ed,comp}}$$

By plotting these three criteria figure 84 is obtained. The thickness of the blade is plotted against the length of the blade. The length of the spring should be above the blue line (criterion 2), below the green line (criterion 3) and between the red solid and the red dashed line (criterion 1). From figure 84 can be concluded that no thickness exist which fulfills all the three criteria.

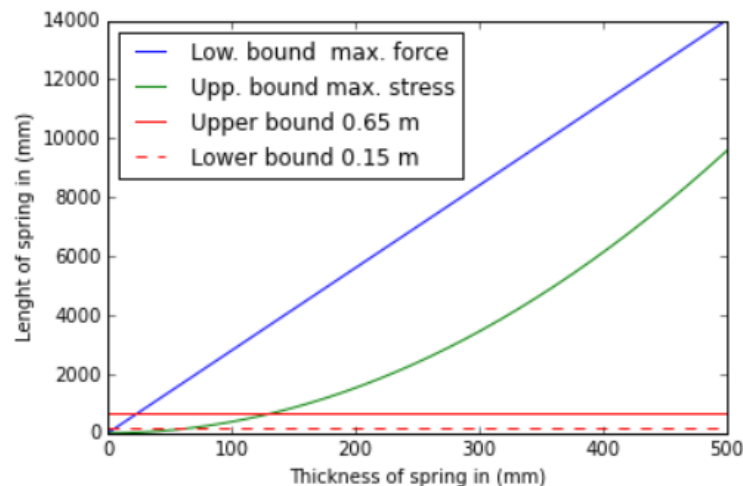


Figure 72 - The upper and lower limits for the thickness and length of the spring

Although the model with the bending beam equations is not accurate since the blade is circular while the bending beam equations do not represent circular beams. In addition the local deformation of the connector is not taken into account. However, from this graph is absolutely clear that the model has to be very inaccurate to find a thickness for the blade which fulfills all the three requirements.

## Appendix E: Reduced area and moment of inertia of the wedge

Here the shear area at the critical location of the wedge is shown.

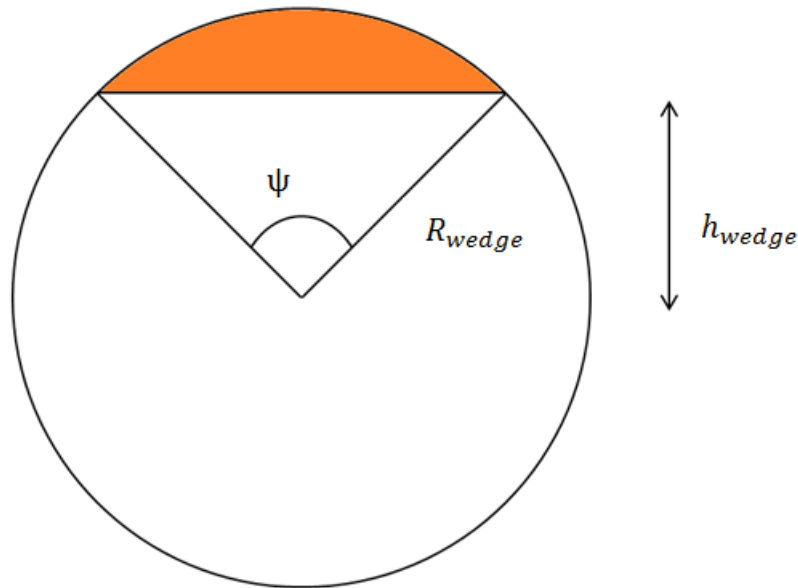


Figure 73 - Shear area at the critical location in the wedge

The shear area at the location of the inclined wedge is given as follows:

$$A_{wedge} = \pi * R_{wedge}^2 - \left( \left( \frac{R_{wedge}^2}{2} \right) * \left( \frac{\psi * \pi}{180} - \sin(\psi) \right) \right), \text{ with } \psi = 2 * \arccos \left( \frac{h_{wedge}}{R_{wedge}} \right)$$

With this  $A_{net}$  the reduction factor for the shear of the full cylinder can be calculated as:

$$r_{A,wedge} = \frac{A_{wedge}}{A_{full,wedge}} \rightarrow A_{wedge} = r_{A,wedge} * A_{full,wedge}$$

The second moment of inertia of the wedge is given by:

$$I_{wedge} = \frac{1}{4} * R_{wedge}^4 \int_{-\psi}^{\frac{\pi}{2}} (1 - \cos(4\psi)) d\psi$$

The maximum bending moment is given by:

$$M_{Rd,wedge} = 1.5 * f_y * W_{el}$$

Since the yield strength is the same, the ratio between the bending moments does only depend on the moment area of inertia. The reduction factor is given by dividing the moment of inertia of the wedge by the moment of inertia of the full circle. This gives:

$$r_{W,wedge} = \frac{\left(\frac{I_{wedge}}{z_{max}}\right)}{\left(\frac{I_{full,wedge}}{R_{wedge}}\right)} \rightarrow W_{el} = r_{W,wedge} * W_{full,wedge}$$